UNIVERSITY OF WISCONSIN-LA CROSSE

Graduate Studies

EFFECTS OF THE *ESCHERICHIA COLI* SMALL REGULATORY RNAS OMRA AND OMRB ON GLOBAL TRANSCRIPTION FOLLOWING GROWTH IN HUMAN URINE

A Manuscript Style Thesis Submitted in Partial Fulfillment of the Requirements for the Degree of Master of Science in Microbiology

Samuel Grund

College of Science and Health
Microbiology

December, 2017

EFFECTS OF THE *ESCHERICHIA COLI* SMALL REGULATORY RNAS

OMRA AND OMRB ON GLOBAL TRANSCRIPTION

FOLLOWING GROWTH IN HUMAN URINE

By Samuel Grund

We recommend acceptance of this thesis in partial fulfillment of the candidate's requirements for the degree of Master of Science – Microbiology.

The candidate has completed the oral defense of the thesis.

William Schwan — 12/8/17

William Schwan, Ph.D., Thesis Committee Chairperson — Date

Scott Cooper — 12/7/17

Scott Cooper, Ph.D., Thesis Committee Member — Date

Marc Rott — 12/6/17

Marc Rott, Ph.D., Thesis Committee Member — Date

John May — 12/8/17

John May, Ph.D., Thesis Committee Member — Date

Thesis accepted

Meredith Thomsen — 1-12-2018

Meredith Thomsen, Ph.D., Graduate Studies Director — Date

ABSTRACT

Grund, S.M. Effects of the *Escherichia coli* small regulatory RNAs OmrA and OmrB on global transcription following growth in urine. MS in Microbiology, December 2017, 55pp. (W. Schwan)

Urinary tract infections (UTIs) are common both in the US and worldwide, with 50-60% of women developing a UTI during their lifetime. The estimated cost of UTIs in the US is 3.5 billion dollars yearly. Approximately 70% - 90% of UTIs are caused by uropathogenic *Escherichia coli* (UPEC). UPEC differentially expresses a variety of genes to establish and maintain UTI in an osmotically stressful, urine-saturated environment. *E. coli* regulates some stress-related genes with small regulatory RNAs (sRNAs). Two sRNAs known to regulate UPEC virulence factors are OmrA and OmrB (OmrAB), which are expressed in high osmolarity conditions. To investigate genes regulated by OmrAB in UPEC grown in human urine, UPEC strains UTI89 and UTI89 Δ*omrAB* were grown in human urine and subjected to RNA sequencing and qRT-PCR analyses. Genes with significantly dysregulated transcript levels in UTI89 Δ*omrAB* were those involved in xylose transport/metabolism (*i.e.*, *xylA, xylR*) as well as the *nhaC* and a *malY* homolog hypothetical protein genes, which encode a putative Na^+/H^+ antiporter and a putative cystathionine β-lyase and maltose operon repressor, respectively. To investigate potential roles these genes have in UPEC survival in urine, UTI89 strains overexpressing *xylR*, *nhaC*, or the *malY* homolog were grown in human urine and compared to the parent strain. Overexpression of *nhaC* and the *malY* homolog significantly decreased and increased UTI89 growth in human urine, respectively. Additionally, overexpression of *xylR* had a minor inhibitory effect on UTI89 growth in human urine. These results indicate novel connections between OmrAB and metabolism and potential virulence factor genes, which could be useful in furthering the understanding of the UPEC transcriptome during a UTI as well as highlighting targets for antibacterial agents.

ACKNOWLEDGEMENTS

I thank my advisor William Schwan and my committee members Scott Cooper, John May, and Marc Rott for their support and assistance during this project. I also thank Jonathan Livny from Broad Institute as well as Henry Schreiber, Matthew Conover, and Scott Hultgren from Washington University for their assistance with the RNA sequencing and analysis. Finally, I thank my family and friends for their support and encouragement throughout my graduate studies.

TABLE OF CONTENTS

PAGE

LIST OF TABLES……..……..……..……...…….. vii

LIST OF FIGURES…..……..……..……..……...……..... viii

INTRODUCTION……..……..……..…… 1

Significance and epidemiology of urinary tract infections……..... 1

Human urinary tract anatomy & physiology……..... 1

UPEC metabolism during UTI……..... 2

Xylose metabolism and operon expression in UPEC……..…. 4

Two-component system regulation in UTI establishment……...… 5

Small regulatory RNAs and virulence…….…… 6

OmrAB and UPEC virulence……..……. 9

Na+/H+ antiporters in bacterial virulence……. 11

Cystathionine β-lyase and maltose metabolism in UPEC virulence……. 12

Objectives……...……...……. 13

MATERIALS AND METHODS…….……..……. 15

Bacterial strains and plasmids…..……..…….. 15

Creation of an *omrAB* deletion in strain UTI89.....…….. 15

RNA extraction for RNA sequencing.....……. 20

RNA extraction and qRT-PCR.....……...……... 21

Xylose detection assay.....……..... 24

Construction of recombinant plasmids.....……... 25

Urine Growth Curves.....……..... 26

RESULTS……..…….…….……... 28

RNAseq analysis……..... 28

qRT-PCR analysis…….. 33

Gene suppression analysis of UTI89 strains in human urine……. 34

Effects of *omrAB* deletion on xylose usage during urine growth ..……...… 37

DISCUSSION…….…….…….……...….. 39

Broad effects of an *omrAB* deletion on the transcriptome of UTI89 grown in urine…….…….…….……..... 40

Effects of *malY* homolog overexpression on UTI89 urine growth……..... 43

Effects of *nhaC* overexpression on UTI89 urine growth……... 45

Effects of *xylR* overexpression on UTI89 urine growth…….……... 46

REFERENCES…….…….…….……...…… 50

LIST OF TABLES

TABLE PAGE

1. Bacterial strains and plasmids used in this study……...… 16

2. Oligonucleotide primers used in this study…… 19

3. Eighty genes exhibiting the most statistically significant transcriptional differences between UPEC strains UTI89 Δ*omrAB* and UTI89 as determined by RNA sequencing……... 29

4. Average read counts of the reference gene *ftsZ* and genes investigated in this study generated by Illumina sequencing-by-synthesis RNA sequencing…….. 33

LIST OF FIGURES

FIGURE PAGE

1. UPEC strategies for survival in human urine……..… 3

2. The *xyl* operons……..……..… 4

3. Targets of OmrA & OmrB relevant to survival of UPEC during a UTI…...… 10

4. Map of the plasmid pKD46…… 17

5. Map of the plasmid pMMB91……..... 17

6. Quantitative reverse-transcribed polymerase chain reaction results of *E. coli* *xylA*, *malY* homolog, *nhaC,* and *fimE* transcription in UTI89 Δ*omrAB* relative to wild-type UTI89 grown in human urine ……..…. 34

7. Growth of UTI89(pSG1), UTI89(pSG2), UTI89(pSG3), and UTI89(pMMB91) in human urine…….…….……. 36

8. Estimated xylose concentrations of UTI89 and UTI89 Δ*omrAB* cultures grown in human urine to mid-log phase (OD_{600} = 0.5) and overnight.……..… 38

9. Nonoxidative pentose phosphate pathway and xylose metabolism…….... 48

INTRODUCTION

Significance and epidemiology of urinary tract infections

Between 50-60% of women will develop a urinary tract infection (UTI) in their lifetime (1, 2). UTIs are the primary cause of ambulatory emergency room visits for women in the U.S, and account for 0.9% of total ambulatory visits. Further, the estimated cost of UTIs in the U.S. is more than 3.5 billion dollars yearly (3). Uropathogenic *Escherichia coli* (UPEC) cause approximately 75% - 90% percent of human UTIs and are responsible for the majority of both community-acquired and healthcare-associated UTIs (4).

Human urinary tract anatomy and physiology

UPEC infections can occur in both the upper and lower urinary tract, and are called pyelonephritis and cystitis/urethritis, respectively. These environments are physiologically and anatomically distinct. The upper urinary tract is composed of the kidneys and ureters. Kidneys are responsible for filtering blood; absorbing various nutrients; regulating pH, fluids, and electrolytes; and producing urine (5). Ureters are muscular tubes that transfer urine to the bladder. In bladder and urethra in both sexes as well as the prostate in males form the lower urinary tract. The bladder is a reservoir for urine and expels it into the urethra, which leads outside the body (6). Additionally, the bladder is the primary site of infection for uropathogens, as about 95% of UTIs occur there (7). Uroepithelial cells line the inner surface of the renal pelvis, ureter bladder, and upper

urethra (8). For UPEC to establish itself in this environment, it must attach to glycosylated uroepithelial cells using pili and survive and grow within a urinary tract saturated with human urine.

Although urine can support bacterial growth, several of its properties can inhibit UTI establishment. For example, urine is generally low in pH, high in osmolality, and flows unidirectionally through the urinary tract, all of which can prevent UTI establishment (9). Human urine can have a pH range between 4 – 8 with an average of pH 6. The specific gravity of human urine ranges from 1.003 – 1.035 with an average of 1.015 (10). A commonly used and robust model for UTI study is the murine urinary tract, which possesses many similarities with the human urinary tract. Murine urine has a pH and specific gravity similar to that of human urine (11), uroplankins (i.e., proteins that coat uroepithelial cells) are conserved between humans and mice (12), and filamentous UPEC cells from human UTI samples were similar to those taken from murine urinary tracts (7).

UPEC metabolism during UTI

Besides pH and osmolality, other UPEC-inhibiting factors of human bladder urine are iron scarcity, moderate oxygenation, and solubilized compounds (13). More than 2,000 different compounds (*e.g.*, urea, salts, proteins, amino acids, oligosaccharides) can be found in human urine that UPEC must utilize or tolerate (14). Normal human urine has Tamm-Horsfall glycoproteins, which inhibit the establishment of a UTI by binding the adhesins of type 1 pili and preventing their attachment to epithelial cells (15). Conversely, small peptides and amino acids are the primary carbon sources for UPEC

during UTI and are relatively abundant in human bladder urine (13, Figure 1). UPEC employs

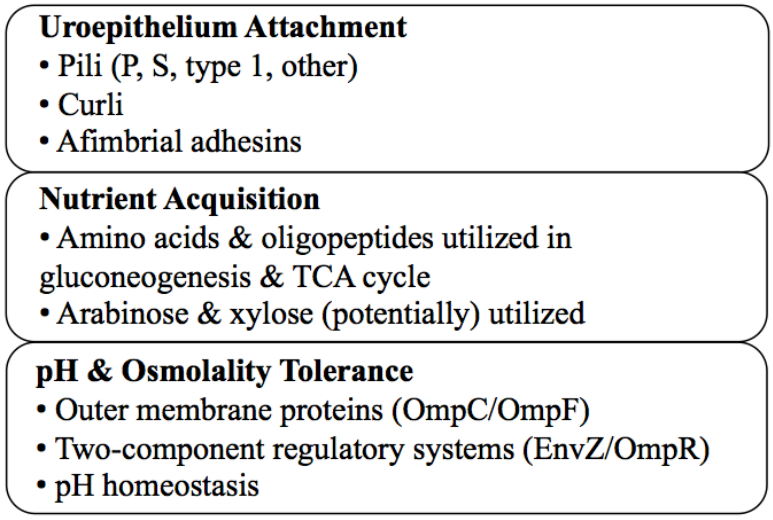


FIG 1 UPEC strategies for survival in human urine.

oligo-peptide and di-peptide binding proteins DppA and OppA, respectively, to import these peptides during UTI, while some amino acids (specifically histidine, serine, arginine, and branched-chain amino acids) are brought into bacterial cells using various permease importers (16). Both DppA and OppA proteins are highly expressed in UPEC grown in urine *in vitro*.

After peptides and amino acids are imported by their respective transporters, they are broken down into oxaloacetate and pyruvate, which are utilized in gluconeogenesis and the TCA cycle, respectively. These two pathways are critical for UPEC fitness during a UTI; however, mutational studies have shown that the disruptions of the pentose phosphate pathway, Entner-Douderhoff pathway, and glycolysis have no detected effect on fitness (13). Although peptides and individual amino acids are the primary carbon source for UPEC, the pentose sugars xylose and arabinose may also be utilized. One

study determined that genes involved in their catabolism are differentially upregulated in urine as compared to iron-limited Luria-Burtani (LB) medium (16).

Xylose metabolism and operon expression in UPEC

The pentose sugar xylose is transported and metabolized by the *xyl* regulon, which includes 2 *xyl* operons containing genes involved in xylose transport (*xylFGH*) and xylose metabolism (*xylAB*) as well as a *xyl* operon transcriptional activator (*xylR*, Figure 2). XylR binds upstream of the *xylAB* and *xylFGH* operon promoters to increase their transcription (17). The *xylFGH* gene products import xylose; specifically, XylF is a xylose-binding protein, XylG is an ATP-binding protein, and XylH is a membrane transporter.

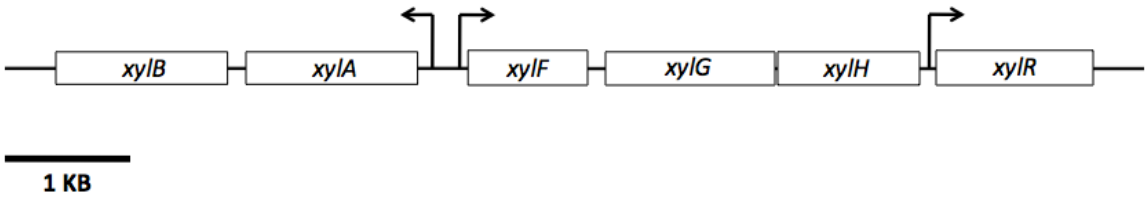


FIG 2 Schematic of the *xyl* operons. Arrows represent transcriptional start sites.

Several studies have shown that the *xyl* regulon is important for UPEC survival. In one study, the *xylFGH* operon was upregulated in an asymptomatic bacteriuria strain when grown in sterile human urine compared to rich growth media (18). The xylose metabolism locus *xylAB* encodes XylA (xylose isomerase), which naturally converts xylose to xylulose but can also convert glucose to fructose (19), and XylB (xylulose kinase), which naturally phosphorylates xylulose to create xylulose-5-phosphate but can also phosphorylate ribose to create ribulose-5-phosphate (20). Transcription of *xylA* was

also upregulated 2- to 5-fold in UPEC strain CFT073 when grown in sterile human urine compared to rich growth media (16). Surprisingly, a CFT073 Δ*xylA* mutant outcompeted the wild-type strain during infection of mouse bladders and kidneys (~60-fold and ~4-fold more mutant cells than wild-type at 48 hours post-innoculation, respectively), although these results were not statistically significant (Wilcoxon matched pairs test P values = 0.0625 and 0.0649, respectively; 16). Moreover, *xylA* transcription was also shown to be downregulated by the two-component regulatory system (TCS) KguR/KguS, which is involved in nutrient acquisition in UPEC strain CFT073 and activated during conditions of low oxygen concentration and high α-ketoglutarate concentration (21).

Collectively, these studies indicate that xylose transport and metabolism genes may be important to UPEC survival during a UTI. This is plausible, as xylose is found in urine in concentrations comparable to those of individual amino acids that are utilized by UPEC during a UTI (*e.g.*, L-serine; mean ~0.3 mM, range 0.04 mM – 1.5 mM) (22), although sugars are less important to UPEC metabolism in urine than amino acids and peptides (13).

Two-component system regulation in UTI establishment

Although nutrient acquisition is an important facet of UTI establishment, UPEC must also tolerate variable and adverse conditions to survive within the human urinary tract. To do this, UPEC employ a variety of TCSs (21). Bacterial TCSs are signal transduction mechanisms that allow cells to respond to environmental stimuli. While functionally diverse, each TCS is composed of two components: a sensor kinase, which senses a stimulus and transmits a signal, and a response regulator, which receives the signal and acts upon its target(s). One TCS important for UPEC survival in the urinary

tract is EnvZ/OmpR, which responds to osmotic stress conditions like those found in human urine. EnvZ, the transmembrane histidine kinase, detects osmotic signals and autophosphorylates itself at histidine 243 (23). This phosphate is then transferred to aspartate 55 of the response regulatory protein OmpR (24), which acts as a transcriptional regulator of target genes. While the specific signal that activates EnvZ is still unknown, different osmolality signals are known to modulate the activity of EnvZ and OmpR (25). Therefore, regulation of OmpR targets, such as the *ompC* and *ompF* porin protein genes, is dependent upon osmolality.

In addition to osmoregulatory functions, OmpR has been shown to regulate genes involved in type 1 pilus synthesis (26, 27), flagella and curli synthesis (28), pH homeostasis, acid response, and biofilm development (29). Moreover, a UPEC Δ*ompR* strain exhibited significantly decreased survival in the murine urinary tract compared to the wild-type strain (26). Transcription of *ompR* was not affected by pH or osmolarity (27). This lack of transcriptional variation is in part due to the promoter sequence of *ompB*, the bicistronic *ompR/envZ* operon (29, 30). Nucleotide differences between the *Salmonella typhimurium* and *E. coli ompB* promoter sequences lead to increased *envZ/ompR* expression in the former and decreased expression in the latter. Because OmpR protein levels were elevated in low pH and high osmolality conditions while *ompR* mRNA levels were not, post-transcriptional regulation must be taking place (27), possibly through the involvement of small regulatory RNAs (sRNAs).

Small regulatory RNAs and virulence

sRNAs are noncoding RNAs that transcriptionally or post-transcriptionally regulate target genes or modify protein function (e.g., RNA polymerase holoenzyme; 31).

The mRNA-targeting sRNAs range in length from 50-500 nucleotides (32) and are categorized into three mechanistically distinct groups. True antisense sRNAs, or *cis*-encoded sRNAs, are reverse complements of their targets that generally repress translation through ribosomal binding site (RBS) blockage or inhibit transcription through base pairing with their target (33). Indeed, these sRNAs can pair completely or incompletely with their target mRNAs, and can be co-transcribed with them from the same locus or transcribed separately from a nearby position. Proteins translated from antisense sRNA-targeted mRNAs can be toxic to cells at high concentrations; in such cases, true antisense sRNAs aid in maintaining appropriate cellular concentrations of these proteins.

The second and better-known class of sRNAs, titled limited complementarity or *trans*-encoded sRNAs, have shorter stretches of reverse complementarity with their targets. *Trans*-encoded sRNAs of enteric bacteria almost always require the chaperone Hfq to mediate pairing with target mRNAs (32). Hfq is a 67 kDa homohexamer with three distinct faces: proximal, distal, and lateral (34). The proximal face binds the poly-uridine tails of sRNAs, while the distal face has a strong affinity for ARN motifs of target mRNAs (where R is a purine and N is any nucleotide). The lateral face contains arginine residues involved in sRNA binding and is required for normal functioning of Hfq (34). Pairing of RNA molecules can have one of two results: increased translational activation (*e.g.,* by putting the transcript in a conformation conducive to ribosomal binding) or translational inhibition (*e.g*., by ribosome-binding site blocking and/or degradation; 32). The *trans*-encoded sRNAs that promote degradation of their targets do so by recruiting the degradosome, a complex of proteins including the ribonuclease RNase E. Like *cis*-

encoded sRNAs, this group of sRNAs generally pairs with the 5' region of its targets. Additionally, *cis*-encoded and *trans*-encoded sRNAs are stoichiometric, meaning that one sRNA molecule regulates a single target mRNA and is degraded with it (31).

The third group of mRNA-targeting sRNAs is Hfq-independent *trans*-encoded sRNAs. sRNAs of this type are generally seen in non-enteric bacteria, such as the Gram-positive species *Bacillus subtilis* and *Staphylococcus aureus* (31). These sRNAs affect their targets similarly Hfq-dependent sRNAs, but they do not associate wth Hfq.

Bacterial sRNAs have been implicated in a wide variety of cellular activities, such as quorum sensing, environmental adaptation, and plasmid replication (34). Additionally, some bacterial sRNAs are involved in virulence within a variety of genera, such as *Vibrio* (Quorum sensing), *Erwinia* (biofilm formation), *Shigella* (acid resistance), and *Klebsiella* (biofilm formation, 35-37). Various *E. coli* sRNAs (*e.g.*, RyhB, RfaH, MicA, and RybB) have also been implicated in virulence. RyhB regulates iron storage control by post-transcriptionally inhibiting non-essential iron-using proteins (38). Since the urinary tract is iron-poor, RyhB is important for UPEC virulence, indicated by a Δ*ryhB* mutant strain exhibiting significantly reduced fitness in the murine urinary tract relative to the wild-type strain (37). MicA regulates the TCS PhoP/PhoQ to affect translation of outer membrane proteins (OMPs) OmpA and LamB (39). MicA has also been shown to promote *E. coli* motility (40) and to post-transcriptionally repress *fimB*, a phase-variation recombinase that promotes type 1 piliation. RfaH, a transcriptional inhibitor and translational activator, indirectly represses MicA and potentially activates unknown inhibitory transcription factors to result in an overall increase in *fimB* expression (38).

The sRNA RybB inhibits translation of OmpA (41), which is involved in adhesion, biofilm formation, and transport, as well as translation the OmpC porin protein (42).

Most Hfq-dependent sRNAs are expressed under stress conditions like high osmolality and nutrient starvation (31, 32). Since both conditions are encountered in the human urinary tract, the OmrA and OmrB (OmrAB) sRNAs appear to be likely contributors to survival in that environment, as they regulate and are induced by the osmoregulator OmpR (29).

OmrAB and UPEC virulence

OmrAB are redundant *trans*-encoded sRNAs that both inhibit and activate translation of target mRNAs in *E. coli* (Figure 3, 43). A microarray analysis of mRNA levels showed OmrAB are involved in the osmotic stress response by regulating the production of outer-membrane proteins such as the OmpT protease, CirA (a siderophore receptor), and EnvZ/OmpR. EnvZ/OmpR activation promotes transcription of *omrAB* while OmrAB post-transcriptionally inhibit EnvZ/OmpR expression, forming a negative feedback loop (29, 43). It has been shown that under acidic conditions, OmpR protein levels increase while transcript levels remain the same, indicating that OmrAB may increase OmpR levels by increasing *ompR* mRNA accessibility to ribosomes (27). Recently, OmrAB levels were shown to be quite sensitive to total levels of OmpR, unlike other robust OmpR targets such as *ompC* and *ompF* that are only sensitive to phosphorylated OmpR (OmpR-P, 29). Furthermore, OmrAB were shown to alter total OmpR levels, while OmpR-P levels remained relatively constant. This provides a mechanism by which OmrAB may regulate a subset of genes affected by OmpR (*i.e.*, by regulating the OmpR targets affected by total OmpR and not OmpR-P). An important

subset of genes that are affected by OmrAB, likely through OmpR, is the *fim* operon (43). This operon contains the *fimA-H* genes, which control type 1 piliation in UPEC (44).

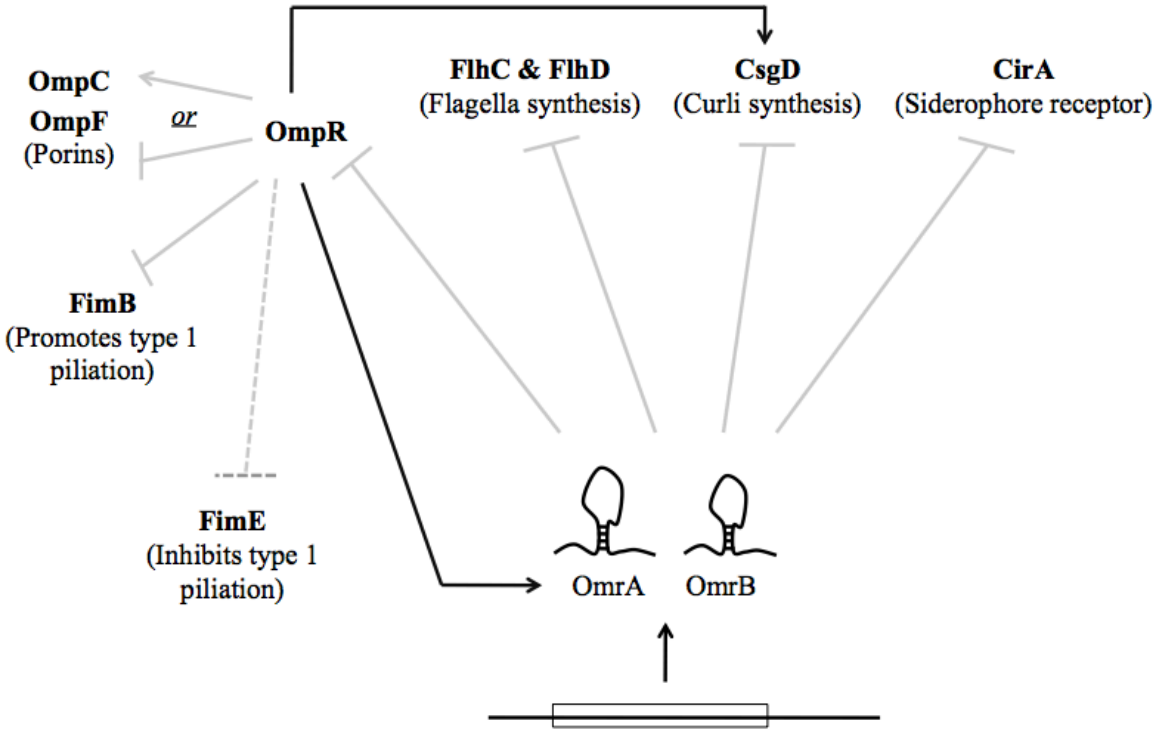


FIG 3 Targets of OmrA & OmrB relevant to survival of UPEC during a UTI. Black lines indicate upregulation of the target, and grey lines indicate repression of the target. The dotted grey line indicates indirect repression of the target.

In addition to EnvZ/OmpR, OmrAB have also been shown to regulate expression of a number of factors involved in UPEC virulence. For example, OmrAB inhibit motility by repressing translation of the *flhDC* mRNA, which encodes a master regulator of flagella synthesis (40). OmrAB also inhibit synthesis of curli proteins, which contribute to virulence through biofilm formation and adhesion (45). OmrAB do this by pairing with a secondary structure in the 5'-UTR of the *csgD* mRNA, which encodes a transcriptional activator of the curli component-producing *csgBA* operon, and inhibiting its expression (46). OmrAB can also inhibit *csgD* transcription indirectly by regulating levels of OmpR

and YdaM, a *csgD* transcriptional activator (47). By regulating flagella and curli synthesis, OmrAB may be allowing cells to focus activity on preservative measures during situations of osmotic stress.

Because OmrAB have been shown to affect expression of genes related to UPEC virulence, it is desirable to investigate other potential roles they may have in virulence. To assess the broad role of OmrAB on UPEC pathways, a double deletion Δ*omrAB* mutant was made in strain NU149. This NU149 Δ*omrAB* strain exhibited reduced fitness in the murine urinary tract relative to the wild-type strain (48). Additionally, several *fim* genes were shown to be dysregulated in NU149 Δ*omrAB* compared to the wild-type strain. These data indicate that OmrAB are important to UPEC *in vivo* and, more specifically, that genes regulated by OmrAB aid UPEC in causing a UTI. Although OmrAB-regulated genes involved in virulence have been discovered, there are likely other genes with undiscovered relationships to OmrAB that are dysregulated in an Δ*omrAB* mutant. Some of these genes may encode proteins in the Na^+/H^+ antiporter superfamily, as one study's microarray results showed the Na^+/H^+ antiporter gene *nhaB* was downregulated by OmrAB (43).

Na^+/H^+ antiporters in bacterial virulence

In general, Na^+/H^+ antiporters are involved in pH and osmolarity tolerance (49). Although utilized by neutrophilic bacteria, they are important to survival in alkaline environments, such as seawater. In acidic environments (*i.e.*, below pH 6.5), some Na^+/H^+ antiporters, such as NhaA, are inactive. However, NhaA is required for full virulence of CFT073 during septicemia in mice, despite many microenvironments within hosts being acidic during sepsis (50). In addition to pH regulation, Na^+/H^+ antiporters can

also be used to regulate osmolarity in pathogens. For example, *Vibrio cholerae* has at least seven Na^+/H^+ antiporters that contribute to its survival in high osmolarity environments (49).

Besides regulating cellular homeostasis, Na^+/H^+ antiporters can also be used to facilitate the transport of molecules through the plasma membrane. For example, some Na^+/H^+ antiporters are involved in drug efflux, while others can transport metabolites such as malate and lactate in and out of cells (49). Interestingly, a protein with both amino acid synthesis and sugar metabolism regulation activity, MalY, may be another UPEC virulence factor.

Cystathionine β-lyase and maltose metabolism in UPEC virulence

As previously mentioned, amino acids and peptides are the main carbon source for UPEC in the urinary tract (13). It has been shown that serine deaminase, which is involved in amino acid metabolism, is important to UPEC growth in urine and *in vivo* (16). Likewise, cystathionine β-lyase, which interconverts cystathionine and homocysteine and is involved in methionine and cysteine metabolism, has been implicated in the virulence of *Salmonella* and *E. coli*. Indeed, a *Salmonella enterica* serovar Typhimurium mutant possessing an inactive *metC* (i.e., the cystathionine β-lyase gene) was attenuated during infection of mouse livers and spleens (51), and *Salmonella enterica* serovar Gallinarum *metC* mutants exhibited significantly inhibited growth in day-old chickens (52). Similarly, a pathogenic avian *E. coli* strain with a *metC* homolog deletion showed reduced fitness relative to the wild-type strain during infection of lungs, livers, and spleens of chickens (53). Additionally, a gene likely homologous to *malY*, which encodes a protein with both cystathionine β-lyase and *mal* regulon repressor

activities, is present on the *metV* pathogenicity island in UPEC strain CFT073 (54). Deletion of the *metV* pathogenicity island resulted in an attenuated mutant in a mouse model relative to the wild-type strain, although other genes were also contained within this region.

Other genes present on the *metV* pathogenicity island include *pafP* and *pafR*. The *pafP* gene encodes a protein that exhibits similarity to the glucose/maltose phosphotransferase system permease *malX*. Immediately downstream of *pafP* is *pafR*, which encodes a transcriptional antiterminator that causes downregulation of the maltose transport and metabolism (*mal*) regulon and regulates other genes (55). It was shown that CFT073 Δ*pafPR*, Δ*pafP*, and Δ*pafR* deletion mutants were each outcompeted by the parent strain in urine, bladder, and kidneys during coinfection of mice. Additionally, there is evidence that connects outer membrane maltoporins to cytopathicity in enteropathogenic *E. coli* (56), growth of Group A *Streptococcus* in saliva to maltose metabolism (57), and virulence factor production with maltose metabolism in *V. cholerae* (58). The presence of the maltose/glucose permease gene *malX* has shown a strong positive correlation with pathogenicity in *E. coli* (59).

Because the *mal* regulon and cystathionine β-lyase both appear to contribute to bacterial virulence in a variety of contexts, a protein that has connections to both pathways may prove to also be tied to virulence. The *malY* gene encodes a protein with activity as a cystathionine β-lyase and *mal* gene repressor and, interestingly, has a homolog in strain UTI89. Immediately downstream of that *malY* homolog is a gene with significant homology to the NhaC family of Na^+/H^+ antiporters.

Objectives

This study investigated how OmrA and OmrB affect the UPEC transcriptome during growth in human urine and whether certain genes with differential expression in a UTI89 **Δ***omrAB* mutant contribute to UPEC survival in human urine. We hypothesize that OmrAB regulate expression of genes involved in xylose metabolism (*xylAB*) and transport (*xylFGH*) during UPEC growth in human urine. Additionally, connections of the *nhaC* and *malY* homolog genes to UPEC growth in human urine were also investigated. This project had three main objectives:

1. Determine the transcriptional differences between UTI89 **Δ***omrAB* and the parent strain grown in human urine using RNAseq of total RNA extracted from both strains.
2. Confirm the RNAseq results using quantitative real-time polymerase chain reaction (qRT-PCR) on RNA populations from UTI89 Δ*omrAB* and the wild-type strain, both grown in human urine.
3. Overexpress genes of interest dysregulated in the UTI89 Δ*omrAB* mutant grown in urine in the UTI89 background and compare each strain's ability to grow in human urine to that of the parent strain.

MATERIALS AND METHODS

Bacterial strains and plasmids

The UPEC strain UTI89 used in this study is a clinical isolate (60) that has had its genome sequenced and available on the open access database GenBank (Table 1, 61). Strain DH5α was used for recombinant plasmid selection and propagation. Plasmid pKD46 (Figure 4) contains the genes encoding the λ Red recombinase ligated to an *ara* promoter, which recombines the gene of interest with an antibiotic resistance gene. The pKD4 plasmid has a kanamycin resistance (Kan^R) marker flanked by FRT sites. Plasmid pCP20 was used to express the FLP recombinase, which recognizes FRT sites and excises the Kan^R marker from the deletion mutant's genome. Both pCP20 and pKD46 have temperature-sensitive origins of replication that are shut off when the temperature gets above 32°C. Plasmid pMMB91 was used for cloning and gene overexpression in suppression analysis studies.

Creation of an *omrAB* deletion in strain UTI89

To create the UTI89 Δ*omrAB* deletion mutant, a modified version of the λ Red recombinase system, originally described by Datsenko and Wanner (62), was used. Strain UTI89(pKD46) was shaken overnight in 3 ml of super optimal broth (SOB) medium with 100 μg/ml ampicillin ($SOB\text{-}Amp^{100}$) at 32°C. One ml of the overnight culture was used to inoculate 50 ml of $SOB\text{-}Amp^{100}$, which was shaken at 250 rpm to an OD_{600} of 0.5 at 32°C. To cure the pKD46 plasmid (Figure 4) from the strain, a 20 ml aliquot of culture was transferred to a sterile flask and incubated at 42°C and 250 rpm for 15 min. Twenty

TABLE 1 Bacterial strains and plasmids used in this study

Strain or plasmid	Description	Reference or source
Strains		
UTI89	UPEC clinical isolate	60
UTI89 Δ*omrAB*	Δ*omrAB* in UTI89 background	This study
DH5α	*supE44, lacU169(lacZΔM15), hsdR17, endA1 gyrA96 thi-1 relA1*	Thermo Fischer Scientific
Plasmids		
pKD46	λ Red recombinase, Amp^R	62
pKD4	FRT-flanked Kan^R cassette, Amp^R	62
pCP20	FLP recombinase, Amp^R	62
pMMB91	Low-copy plasmid, *tac* promoter, Kan^R	63
pSG1	pMMB91::*xylR*	This study
pSG2	pMMB91::*malY*	This study
pSG3	pMMB91::*nhaC*	This study

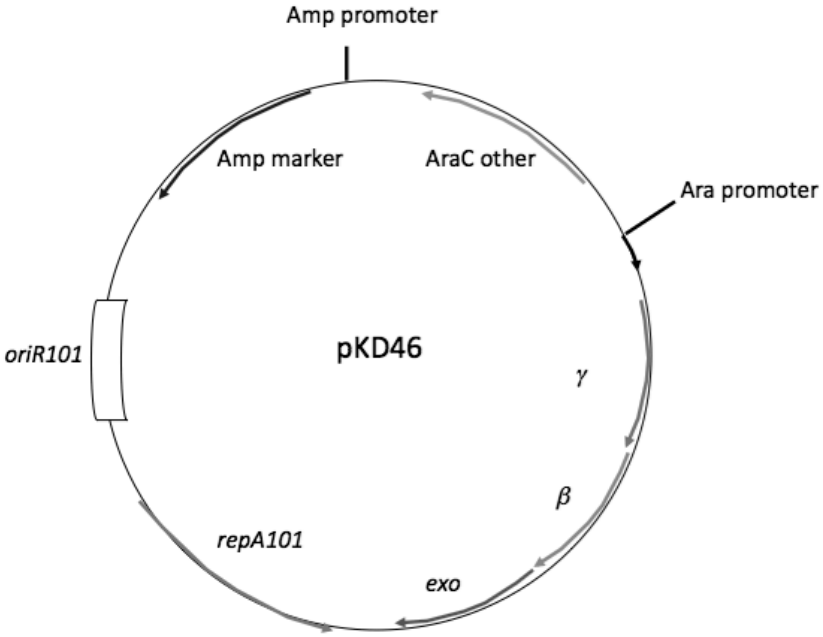


FIG 4 Map of the plasmid pKD46.

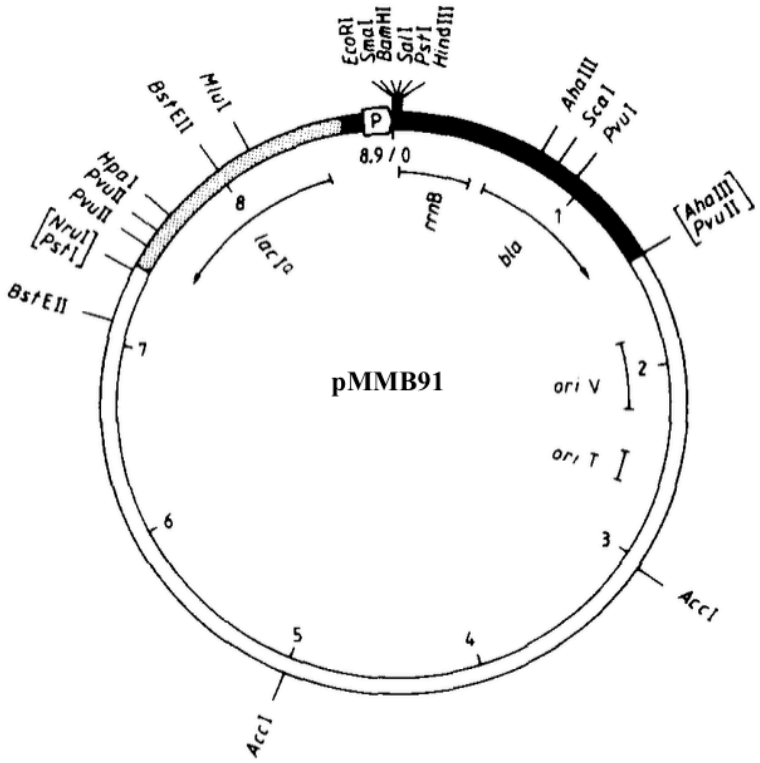


FIG 5 Map of the plasmid pMMB91.

ml of culture was then pelleted by centrifugation for 10 min at 4°C and 8,000 *x g*. Cell pellets were washed three times with 5 ml of ice cold, sterile, distilled water, and resuspended in 200 µl of sterile water. Eighty µl of cells were put into a 0.2 cm electroporation cuvette (BioRad, Hercules, CA) and combined with 1/10 vol (~1-2 ug DNA) of the PCR product.

The PCR product that was electroporated with the cells was created using primers (OmrAB3/4, Table 2) that target the Kan^R marker on the pKD4 plasmid. The ends of these primers have homology with the ends of the gene of interest, which allow for recombination, as well as FRT sites (*i.e.*, FLP recombinase sites), which are required for subsequent excision of the Kan^R marker from the genome. The pKD4 plasmid was used as a template in each PCR reaction, which contained 100 pM oligonucleotide primers, one µl of template DNA, 500 nM dNTP, 20 µl of Complete Wigler's Buffer (67 mM tris-HCl pH 8.8, 4 mM $MgCl_2$, 16 mM $(NH_4)_2SO_4$, 10 mM β-mercaptoethanol, 100 µg/ml bovine serum albumin; 64), and 5 U of GoTaq Flexi DNA polymerase (Promega, Madison, WI) in a 100 µl volume. The reaction conditions consisted of an initial denaturation at 95°C for 5 min, followed by 35 cycles at 95°C for 1 min, an appropriate annealing temperature for 1 min, and 72°C for 1 min. The DNA was precipitated overnight at -20°C using two volumes of 100% ethanol and 1/10 volume of 3 M anhydrous sodium acetate (Merck, Darmstadt, Germany), resuspended, purified via gel electrophoresis, precipitated, and resuspended in 40 µl of water.

The cells were electroporated with the DNA for 5 ms under the following conditions: capacitance, 100 Ω; resistance, 25 µF; and charging voltage, 2.5 kV. The electroporated cells were immediately recovered in 1 ml of super optimal broth with

TABLE 2 Oligonucleotide primers used in this study

Primer	Gene	Sequence (5' → 3')[a]
EcFtsZ1	*ftsZ*	TAGCGGTATCACCAAAGGACT
EcFtsZ2		GTGATCAGAGAGTTCACATGC
OmrAB3	*omrAB*	**TTACACGAGATAAAGAACGCGAGCGACAGTAAATTAGGTGCG**TGTGTAGGCTGGAGCTGCTTCG
OmrAB4		ACC**GCTGGTGGCGTTTGGCTTCAGGTTGCTAAAGTGGTGATC**ATATGAATATCCTCCTTAG
OmrA9	*omrA*	GGTGAGATTATTCGCTACGCT
OmrA10		ACCCGTAACGCGAACGCGAT
XylR1	*xylR*	TCAATGCCAATAAAGCCTATG
XylR2		GTAATGAACGGGTAACTTTC
XylR5		ACAGAATTCTGATTCAGCAGGAAAAGAACC
XylR6		ACAGGATCCCGACGCCGATAATTCTCATCA
XylA1	*xylA*	CAAGCAATACTTCCGAGTTTTAGG
XylA2		TTTGAGTTTACGCTGTAGAC
MetC5	*malY*	ACAGAATTCATCGGGCGAGTAACAAATATG
MetC6		ACAGGATCCGGGGATCTTGGAGTATTGTTA
NhaC1	*nhaC*	CTCTGGTGGAATCATTATTACC
NhaC2		GGAATAGTACCGCCTATCATC
NhaC5		ACAGAATTCCACTACAGGAGTTTCCCTTC
NhaC10		ACAGTCGACATCAGGCCGATTCTATTTGCT

[a] Restriction endonuclease sites are underlined, homologous ends of OmrAB primers are in bold.

catabolite repression (SOC) medium and were shaken at 250 rpm for 1 h at 37°C.

Transformed cells were plated onto Luria agar (LA) with 40 μg/ml kanamycin and incubated overnight at 37°C. Transformants were patched onto LA with 40 μg/ml kanamycin as well as LA with 100 μg/ml ampicillin and were incubated at 37°C. A patched colony with a Kan^R, Amp^S phenotype was subcultured and electroporated as described above with ~20 ng of pCP20. Each deletion mutant had the pCP20 plasmid cured by growth at 42°C. The Δ*omrAB* deletion was confirmed via a PCR reaction targeting the 5'-UTR and 3'-UTR of the *omrAB* genes. Each PCR reaction contained 50 pmol oligonucleotide primers (OmrA9/10, Table 2), 1 μl of a chromosomal DNA aliquot from the putative UTI89 Δ*omrAB* strain, 500 nM dNTP, 10 μl of Complete Wigler's Buffer (64), and 3 U of GoTaq Flexi DNA polymerase (Promega; Madison, WI) in a 50 μl volume. Negative and positive control reactions were also performed, which contained either ddH_2O or UTI89 chromosomal DNA, respectively.

RNA extraction for RNA sequencing

Once the UTI89 Δ*omrAB* strain was created, it was sent to the Scott Hultgren laboratory at Washington University to be used in RNA extraction and RNAseq. Extraction of RNA samples from strains UTI89 and UTI89 Δ*omrAB* was performed as follows. First, midstream urine pooled from at least two individuals was sterilized using a Stericup 0.22 μm vacuum filter (EMD Millipore, Billerica, MA). Strain UTI89 and UTI89 Δ*omrAB* were inoculated into 3 ml LB broth and grown overnight at 37°C and 250 rpm. Forty ml aliquots of sterile human urine were then inoculated to 1% total volume using the overnight cultures and incubated at 37°C and 250 rpm. After the cultures were grown overnight (~16 h), they were pelleted at 8,000 *x g* for 10 min. The

cells were resuspended in 400 μl sterile H_2O and treated with 2.5 mg/ml lysozyme (Thermo-Fisher Scientific, Waltham, MA) for 30 min at 37°C. The lysed cultures were then mixed with 500 μl of 65°C TRIzol reagent (Thermo-Fisher Scientific, Waltham, MA) and incubated at room temperature for 5 min, after which the protein was pelleted by centrifugation at 12,000 *x g* for 1 min. After the phase separation, RNA from the aqueous phase was purified using the Zymo Research DirectZol kit (Irvine, CA) according to the manufacturer's instructions. The Zymo Research clean and concentrate kit was used to remove DNA from samples. Three replicate sets of DNA-free RNA samples were used in next generation RNAseq performed using a HiSeq2500 Illumina machine (Illumina, San Diego, CA), which utilizes a sequencing-by-synthesis technology. Annotation was performed by Jonathan Livny from the Broad Institute at MIT and Harvard. The annotated data was put into an Excel file and given to our laboratory via email.

RNA extraction and qRT-PCR

To confirm the RNAseq results, a quantitative real-time polymerase chain reaction (qRT-PCR) technique was used to further investigate transcript abundance of genes identified by the RNAseq results as being differentially regulated in the Δ*omrAB* mutant culture compared to wild-type culture after growth in human urine. Twenty-five ml aliquots of filter-sterilized urine were inoculated with a UTI89 or UTI89 **Δ***omrAB* colony and grown overnight (~16 h) at 37 °C, 250 rpm. Cultures were pelleted by centrifugation at 8,000 *x g*, 4°C for 10 min, and the supernatant was removed by aspiration. Total RNAs were extracted using the RNAsnap method as described by Stread *et al.* (65), which first entails cell lysis at 95°C for 7 min in 1 ml of a reagent containing

91% RNA-grade formamide (Sigma-Aldrich, St. Louis, MO), 18 mM EDTA (Thermo-Fisher Scientific, Waltham, MA), 0.025% SDS (Thermo-Fisher Scientific, Waltham, MA), and 1% β-mercaptoethanol (Sigma-Aldrich, St. Louis, MO). The samples were mixed with 1 volume 0.1% DEPC-treated H_2O, and a phenol-chloroform extraction was performed by adding 1 volume of buffered phenol (Sigma-Aldrich, St. Louis, MO) and 1 volume chloroform (Thermo-Fisher Scientific, Waltham, MA). Samples were mixed by inversion, pelleted by centrifugation at 14,000 *x g* for 10 min, and the aqueous phase was transferred to a new microfuge tube without disturbing the protein pellet. An equal volume of chloroform (Thermo-Fisher Scientific, Waltham, MA) was added, and the samples were mixed, centrifuged, and transferred as described earlier in this paragraph. Samples were precipitated at -80°C for at least 1 h using 2.5 volumes of 100% ethanol and 1/10 volume of 0.1% DEPC-treated 3M sodium acetate. RNA samples were pelleted by centrifugation at 14,000 *x g* and 4°C for 15 min, and the supernatant was decanted. The RNA pellets were washed with 70% ethanol in 0.1% DEPC-treated water, pelleted by centrifugation at 14,000 *x g* and 4°C for 5 min, decanted, and air-dried in a biosafety cabinet for 20 – 30 min. Pellets were then resuspended in 50 μl of 0.1% DEPC-treated water and incubated with 30 U RNase-free recombinant DNase I (Life Technologies, Carlsbad, CA) for 1 h at 37°C. A subsequent phenol-chloroform extraction and precipitation was performed as previously described.

To assess RNA quality, A_{260} and A_{280} measurements were taken using a Nanodrop 2000 spectrophotometer (ThermoFischer, Waltham, MA), A_{260}/A_{280} ratios were calculated, and 1 μg aliquots of each RNA sample were analyzed for rRNA bands via 0.8% agarose gel electrophoresis with TBE buffer. An A_{260}/A_{280} ratio of ~2.0 in

addition to clear 5S, 16S, and 23S rRNA bands were used to judge high quality. To check for genomic DNA (gDNA) contamination, RNA samples were used as templates in PCR reactions that contain the following components: 50 pmol of primers EcFtsZ1/2 (which target the housekeeping gene *ftsZ*, Table 2), ~100-200 ng of an RNA sample, 500 μM dNTPs, 10 μl of Complete Wigler's Buffer (64), and 3 U GoTaq Flexi DNA polymerase (Promega, Madison, WI) in a 50 μl volume. The reaction conditions consisted of initial denaturation at 95°C for 5 min, followed by 30 cycles at 95°C for 1 min, 57°C for 1 min, and 72°C for 1 min. No product was observed after 1.5% agarose gel electrophoresis if the RNA sample was free from significant chromosomal DNA contamination.

After confirming the quality of RNA samples, 1 μg of total RNA was used to create cDNA with a Superscript III First-Strand Synthesis kit (Life Technologies, Carlsbad, CA) according to the manufacturer's instructions. To investigate transcription levels of genes potentially regulated by OmrAB, qRT-PCR was performed using the LightCyler FastStart DNA MASTER^{plus} SYBR Green kit (Roche, Basel, Switzerland) on genes potentially differentially transcribed in the UTI89 Δ*omrAB* mutant strain compared to the wild-type strain. Twenty microliter reactions were made using 2 μl of SYBR green master mix, 50 pmol of each oligonucleotide primer, 2 μl of cDNA, and PCR-grade water. Primer pairs targeting *xylA* (XylA3/4), *nhaC* (NhaC1/2), and the *malY* homolog (MetC1/2) were used (Table 2). The reaction conditions consisted of an initial denaturation at 95°C for 3 min, followed by 35 cycles at 95°C for 30 sec, 57°C for 30 sec, and 72°C for 30 sec. As a reference control, the EcFtsZ1/2 primer pair (Table 2) were used. All qRT-PCR was performed in a CFX96 Touch Real-Time PCR Thermocycler (BioRad, Hercules, CA). A minimum of three replicate reactions were

performed for each gene using two different total RNA sets. Transcriptional differences were calculated using the crossover points of each sample according to the method shown below (66, 67), with Ct being the crossover point of a particular cDNA sample, *ftsZ* indicating the housekeeping gene, G.O.I. indicating the gene of interest, and R being the fold-difference in transcription between strains.

$$R = \frac{2^{Ct(FtsZ)}}{2^{Ct(G.O.I)}} \div \frac{2^{Ct(FtsZ)}}{2^{Ct(G.O.I)}}$$

UTI89 UTI89 mutant

To confirm the validity of the qRT-PCR results, various templates were used in control reactions: UTI89 chromosomal DNA was used in positive control reactions, *Staphylococcus aureus* chromosomal DNA was used in negative control reactions, and water was used in no template control reactions. Transcription levels of *ftsZ* were used to normalize transcription levels of targeted genes in each run. All primers were purchased from Integrated DNA Technologies (Coralville, IA). Results were analyzed using a paired two-tailed Student's t-test. Any P value < 0.05 was considered significant.

Xylose detection assay

To compare xylose use in UTI89 Δ*omrAB* versus the wild-type strain, an assay measuring xylose in human urine (69) that was recently modified for increased sensitivity (70) was used. When xylose is heated to 95 - 100°C with hydrochloric acid, it is converted to furfural (71). Furfural reacts with phloroglucinol to produce a stable red-colored product that absorbs at a wavelength of 554 nm, which is measurable. A color reagent composed of 0.5 g phloroglucinol (Sigma-Aldrich, St. Louis, MO), 100 mL of

glacial acetic acid, and 10 ml HCl, was prepared. Five hundred μl of urine culture containing UTI89 Δ*omrAB* or the parent strain was pelleted by centrifugation at 17,000 *x g* for 1 min to remove cells, and 25 μl of sterile urine or urine culture supernatant were combined with 25 μl aliquots of sterile deionized water and 950 μl volumes of phloroglucinol reagent in microfuge tubes. Tubes were incubated at 100°C for 4 min in a heat block, then cooled to room temperature in water. Absorbance readings at 554 nm were measured in a Shimadzu Bio-Spec 1601 spectrophotometer. To determine a test sample's xylose concentration, the sample readings were converted to mg/l values using an equation generated by a standard curve of xylose samples with known concentrations of 0.125, 0.25, 0.5, 1.0, 2.0, 4.0, and 5.0 mg/l.

Construction of recombinant plasmids

The *xylR* and hypothetical protein genes *malY* homolog and *nhaC* were amplified from UTI89 chromosomal DNA via PCR consisting of an initial denaturation at 95°C for 5 min, followed by 32 cycles at 95°C for 1 min, 61°C for 1 min, and 72 °C for 1.5 min. Each reaction contained 50 pmol of each primer, 1 μl of UTI89 gDNA, 500 μM dNTP, 10 μl of Complete Wigler's Buffer (64), and 3 U GoTaq Flexi DNA polymerase in a 50 μl volume. The primer sets used to amplify fragments for cloning into pMMB91 were XylR5/6, MetC 5/6, and NhaC5/10. Each primer set was flanked by *Eco*RI and *Bam*HI (XylR5/6 and MetC5/6) or *Eco*RI and *Sal*I (NhaC5/10) restriction endonuclease sites.

The PCR products were precipitated as described above and resuspended in 50 μl ddH_2O. Twenty microliters of DNA were digested with 20 U of each restriction enzyme according to manufacturer's instructions (New England Biolabs, Ipswich, MA) overnight at 37°C. Plasmids DNA was extracted from an overnight culture of DH5α(pMMB91)

cells using a QiaPrep spin mini-prep kit (Qiagen, Valencia, CA) and a 40 μl aliquot of pMMB91 was subjected to the same digestion conditions as their corresponding DNA fragment. Digestion reactions were heat-inactivated at 65°C for 20 min and precipitated as previously described. Digested DNA fragments and plasmids were ligated using 1 μl T_4 DNA ligase in 1X T_4 DNA ligase buffer (New England Biolabs, Ipswich, MA) according to the manufacturer's instructions (72). The recombinant plasmids were transformed into DH5α using $CaCl_2$ transformation. Briefly, 100 μl of competent DH5α was mixed with 10 μl ligation reaction, incubated at 42°C for 30 sec, added to 1 ml of SOC medium, and incubated at 37°C with shaking at 250 rpm for 1 h. Transformed cells were plated on LA + 40 μg/ml kanamycin. Transformants were checked for recombinant plasmids by plasmid extraction and digestion with appropriate restriction endonucleases as previously described. Digested plasmid DNA was analyzed via 0.8% agarose gel electrophoresis in TBE buffer. All recombinant plasmids were introduced into UTI89 by electroporation as described above. The generated recombinant plasmids harbored *xylR*, the *malY* homolog, or *nhaC*, and were named pSG1, pSG2, and pSG3, respectively.

Urine Growth Curves

To investigate how each deletion mutation in strain UTI89 affected growth in human urine, urine growth curves were performed using the wild-type and suppression analysis strains comparing the UTI89 mutants to their respective parent strains. Three milliliter aliquots of LB broth were inoculated with a mutant or wild-type UTI89 strain and incubated overnight at 37°C with shaking at 250 rpm. Midstream, clean catch urine (IRB approval) was pooled from two or more healthy adults, including at least 1 female, and filter-sterilized using a Stericup 0.22 μm vacuum filter (EMD Millipore, Billerica,

MA). The pH and specific gravity were recorded using an Orion Star A211 pH meter (Thermo-Fisher Scientific, Waltham, MA) and a Reichert TS400 total solids refractometer (Depew, NY), respectively. Overnight LB broth cultures were used to inoculate 25 ml aliquots of sterile human urine to an average OD_{600} of 0.010. Cultures were incubated in 125 ml Erlenmeyer flasks with shaking at 250 rpm and 37°C for 24 h. OD_{600} measurements were taken using a Nanodrop 2000 spectrophotometer and 1 cm plastic cuvettes every two hours from 0-12 h post-inoculation, followed by final measurements taken at 24 h. At least three experimental replicates were performed for each strain being investigated on separate days. Unpaired two-tailed Student's t-tests were performed, testing the mean OD_{600} values of each mutant strain at each time point relative to the mean density of the parent strain at each time point with any P value < 0.05 being considered significant.

RESULTS

RNAseq analysis

Illumina RNAseq was performed by the Scott Hultgren laboratory at Washington University using three replicate RNA samples isolated from UTI89 and UTI89 Δ*omrAB* cultures incubated at 37°C shaken and 250 rpm overnight (~16 h) in filter-sterilized human urine. A total of 408 genes exhibited significantly different transcript levels between the strains according to adjusted P values calculated using DESeq2, with 205 genes being significantly upregulated and 203 genes being significantly downregulated in UTI89 Δ*omrAB* relative to the parent strain. Eighty genes with the lowest P values (*i.e.*, the most significant differential expression between strains) are provided (Table 3). Of these 80 genes, 20 are associated with carbohydrate metabolism, 20 are hypothetical or unannotated, 20 genes are associated with amino acid transport and metabolism (*e.g.*, the isoleucine-valine *ilv* operon and the glutamate *glt* operon), 7 genes are prophage-related, and 12 genes are related to housekeeping functions (*e.g.,* rRNA or DNA polymerase genes). Genes exhibiting the largest difference in transcript abundance in strain UTI89 Δ*omrAB* relative to the wild-type strain included 6 associated with the *xyl* operons as well as 2 annotated as hypothetical protein genes, 1 encoding a Na^+/H^+ antiporter (*nhaC*), and the other encoding a protein homologous to the cystathionine β-lyase and *mal* operon regulator *malY* (*malY* homolog, Table 3). Each of these mRNAs had significantly higher average read counts in UTI89 Δ*omrAB* relative to the parent strain while the housekeeping gene *ftsZ* exhibited similar read counts in both strains (Table 4).

TABLE 3 Eighty genes exhibiting the most statistically significant transcriptional differences between UPEC strains UTI89 Δ*omrAB* and UTI89 as determined by RNA sequencing.

Gene	Product	Fold-difference [a]
Carbohydrate transport, metabolism		
xylA	Xylose isomerase	23
xylR	Xylose operon regulator	14
xylB	Xylulose kinase	13
xylF	Xylose transporter, subunit	122
xylG	Xylose transporter, ATP-binding subunit	39
xylH	Xylose permease	30
yicI	α-xylosidase	7.2
yicJ	Inner membrane Na^+:carbohydrate symporter	13
manX	PTS system mannose-specific transporter subunit IIAB	-2.5
manY	Mannose phosphotransferase system subunit IIC	-2.2
manZ	Mannose phosphotransferase system subunit IID	-2.7
malT	Maltose regulon transcriptional regulator	-1.6
araF	L-arabinose-binding periplasmic protein	-1.8
uhpA	Transcription factor, *uhpT*	2.7
uhpB	Signal transduction kinase, hexose phosphate transport	3.1
rbsA	D-ribose transporter ATP binding protein	2.1
yiaK	2,3-diketo-L-gulonate reductase	-1.9
yiaL	2,3-diketo-L-gulonate utilization	-2.4
bglJ	*bgl* operon transcriptional activator	2.2
yabN	Transcriptional regulator SgrR; sRNA *sgrS* activator	1.8
ycgC	Dihydroxyacetone kinase subunit M	2.6
ycgS	Dihydroxyacetone kinase subunit L	-1.9
ycgT	Dihydroxyacetone kinase subunit K	-2.0

TABLE 3 (Continued)

Gene	Product	Fold-difference [a]
Hypothetical proteins		
nhaC	Na^+/H^+ antiporter	65
malY homolog	Cystathionine β-lyase and maltose operon repressor	100
bax	Hypothetical protein	2.2
ydcH	Hypothetical protein	-2
ykgG	Hypothetical protein	-1.7
ytfK	Hypothetical protein	-1.9
yqiC	Hypothetical protein	-1.7
ykgE	Hypothetical protein	-2.0
yahO	Hypothetical protein	-2.5
ucpA	Short chain dehydrogenase	-1.9
C0399	Hypothetical protein	-2.6
C0959	Prophage CP-933T hypothetical protein	2.5
C0961	Hypothetical protein	2.3
C0962	Hypothetical protein	2.2
C1516	Hypothetical protein	2.4
C2016	Hypothetical protein	-2.2
C4256	Hypothetical protein	2.0
C4811	Hypothetical protein	-2.2
C4813	3-ketoacyl-ACP reductase	-2.2
C4979	Hypothetical protein	2.4

TABLE 3 (Continued)

Gene	Product	Fold-difference [a]
Amino acid transport, metabolism		
ilvG	Acetolactate synthase 2 subunit	2.5
ilvM	Acetolactate synthase 2 subunit	2.1
ilvB	Acetolactate synthase subunit	1.8
ilvN	Acetolactate synthase subunit	2.0
ilvC	3-ketol-acid reductoisomerase	2.7
ilvA	Threonine dehydratase	2.1
ilvE	Branched-chain amino acid aminotransferase	2.0
ilvD	Dihydroxy-acid dehydratase	2.1
thrL	*thr* operon leader peptide	-2.3
nadB	L-aspartate oxidase	1.9
leuD	Isopropylmalate isomerase small subunit	1.7
glnA	Glutamine synthetase	2.6
gltJ	Glutamate ABC transporter	2.1
gltK	Glutamate/aspartate transport system permease	2.5
gltL	ATP-binding protein of glutamate/aspartate transport system	2.2
ddl	D-alanyl-alanine synthetase A	-1.6
ykgF	Electron transport protein	-1.9

TABLE 3 (Continued)

Gene	Product	Fold-difference [a]
Phage-related		
pspA	Phage shock protein	-2.6
pspB	phage shock protein B	-2.3
pspC	DNA-binding transcriptional activator	-2.2
pspD	peripheral inner membrane phage-shock protein	-2.4
pspE	thiosulfate:cyanide sulfurtransferase	-1.8
pspG	Phage shock protein G	-2.7
ybcQ1	lambdoid prophage DLP12 antitermination protein Q-like protein	-1.9
Housekeeping		
nac	nitrogen assimilation transcriptional regulator	1.9
rib	3,4-dihydroxy-2-butanone 4-phosphate synthase	-2.5
cspE	Cold shock protein	-1.9
pheT	phenylalanyl-tRNA synthetase subunit b	-1.6
ppiC	peptidyl-prolyl cis-trans isomerase C	2.5
lpxC	UDP-3-O-acyl N-acetylglucosamine deacetylase	-1.9
rho	transcription termination factor	2.0
rhoL	rho operon leader peptide	2.1
rpsV	30S ribosomal subunit S22	-2.0
rplT	50S ribosomal protein L20	-1.8
rpmI	50S ribosomal protein L35	-2.0
dnaX	DNA polymerase III subunits g and τ	-1.7
adk	Adenylate kinase	2.0

[a] Fold-difference in transcript abundance, UTI89 Δ*omrAB* vs. UTI89.

TABLE 4 Average read counts of the reference gene *ftsZ* and genes investigated in this study generated by Illumina sequencing-by-synthesis RNA sequencing.

Gene	Average read count (mRNA)	
	UTI89	UTI89 Δ*omrAB*
ftsZ	1,514	1,448
xylA	1,051	38,961
xylR	96	1,935
nhaC	113	15,798
malY homolog	63	15,421

qRT-PCR analysis

To confirm the RNAseq transcript levels of the selected genes during growth in human urine, qRT-PCR was performed using RNA extracted from UTI89 and UTI89 Δ*omrAB* grown in sterile human urine overnight as previously described. Primers targeting the type 1 pili regulatory protein gene *fimE*, as well as the *xylA*, *nhaC*, and *malY* homolog genes, were used to detect their respective transcript abundance. Two-tailed Student's t-tests using ΔC_t values indicated significant differences in transcript levels between the two strains for all genes tested except *fimE* (*fimE*, 2.0-fold, P = 0.30; *xylA*, 1.5-fold, P = 0.035; *malY* homolog, 2.3-fold, P = 0.033; *nhaC*, 2.2-fold, P = 0.0067; Figure 6). The differences in transcript abundance between both strains were inverted (*i.e.*, UTI89 had higher transcript levels) and less drastic relative to the RNAseq data; nonetheless, the Δ*omrAB* mutation caused significant fold-decreases in transcript levels of three genes when compared to the wild-type strain.

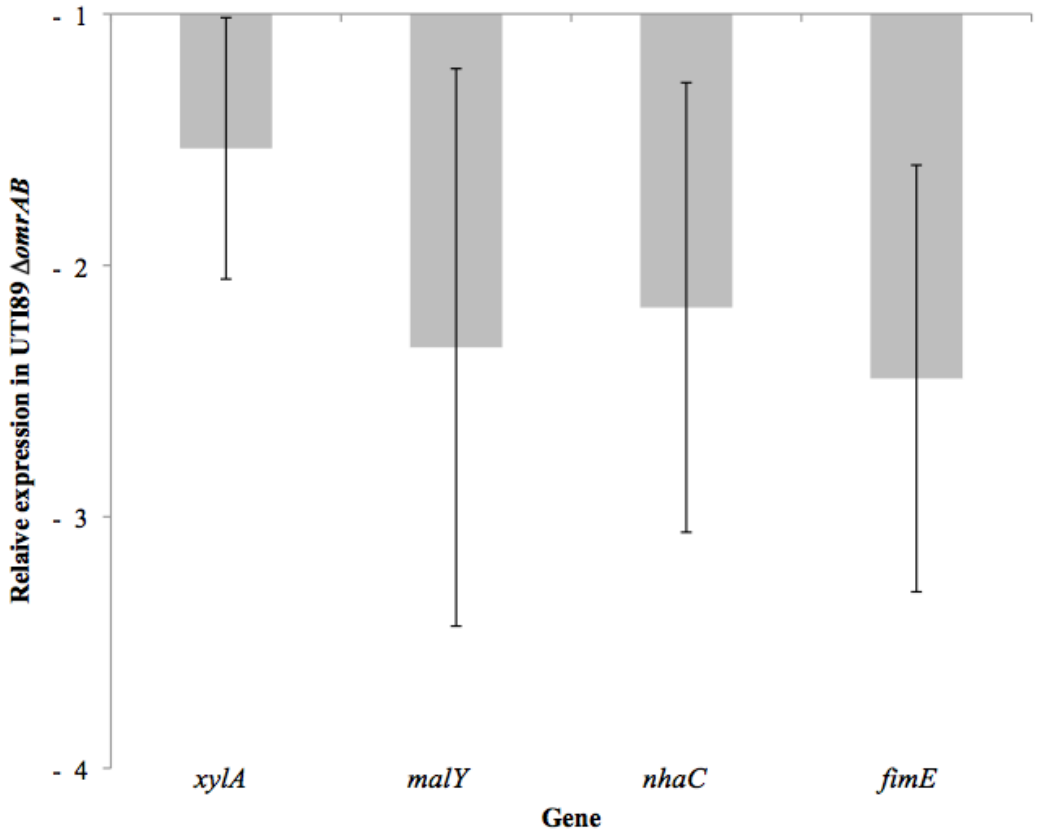


FIG 6 Fold-differences of *E. coli xylA*, *malY* homolog, *nhaC,* and *fimE* transcript levels in UTI89 Δ*omrAB* relative to wild-type UTI89 grown in human urine. Fold-differences were calculated using the $2^{-\Delta\Delta Ct}$ method with *ftsZ* used as the reference gene. The data represents the means ± SD from 3 separate runs, except *fimE* that had only 2 runs.

Gene suppression analysis of UTI89 strains in human urine

After using qRT-PCR to confirm the differences in transcript abundance of several genes in a UTI89 Δ*omrAB* culture relative to the parent strain culture, the effects of those genes on UTI89 growth in human urine were examined. To accomplish this, the *xylR*, the *malY* homolog, and *nhaC* genes were cloned into the low-copy plasmid pMMB91 (named pSG1, pSG2, and pSG3, respectively). UTI89 cultures containing each of the suppression analysis plasmids were grown in sterile filtered pooled human urine and compared to the parent strain harboring pMMB91 (Figure 7). Significant growth reduction was observed in the UTI89 culture overexpressing *nhaC* at the 4 h (P = 0.030),

6 h (P = 0.00002), 8 h (P = 0.0061), and 10 h (P = 0.041) time points relative to the UTI89 parent strain culture. Conversely, UTI89 cultures overexpressing the *malY* homolog exhibited significantly enhanced growth compared to parent strain cultures at 6 h (P = 0.009) and 8 h (P = 0.048). UTI89 cultures overexpressing *xylR* only exhibited significantly enhanced growth relative to the parent strain culture at the 6 h time point (P = 0.038). Together, these results indicate that all three gene products affected UTI89 growth in human urine at certain times, although the *malY* homolog and *nhaC* had a more pronounced effects on strain UTI89 cultures when overexpressed.

Effect of OmrAB deletion UTI89 xylose usage during urine growth

It was expected that, because OmrAB appear to affect *xyl* gene expression, the presence of xylose in urine would be affected by an Δ*omrAB* mutation. To investigate the potential effect of an Δ*omrAB* mutation on xylose usage, UTI89 and UTI89 Δ*omrAB* cultures were grown in urine overnight and the xylose concentrations of culture supernatants were tested by a colorimetric assay utilizing phloroglucinol (70). Supernatants of mid-log phase and stationary phase overnight cultures as well as sterile urine were each combined with acidic phloroglucinol reagent to measure the xylose concentration in each sample. The sterile urine had an estimated mean xylose concentration of 1.73 mg/l, while supernatants of mid-log phase cultures of UTI89 and UTI89 Δ*omrAB* had estimated mean xylose concentrations of 0.832 mg/l and 0.923 mg/l, respectively (Figure 8). Additionally, UTI89 and UTI89 Δ*omrAB* overnight urine culture supernatants had estimated mean xylose concentrations of 0.797 mg/l and 0.784 mg/l, respectively. Significant differences in estimated xylose concentrations were observed when sterile urine was compared with supernatant from either of the cultures

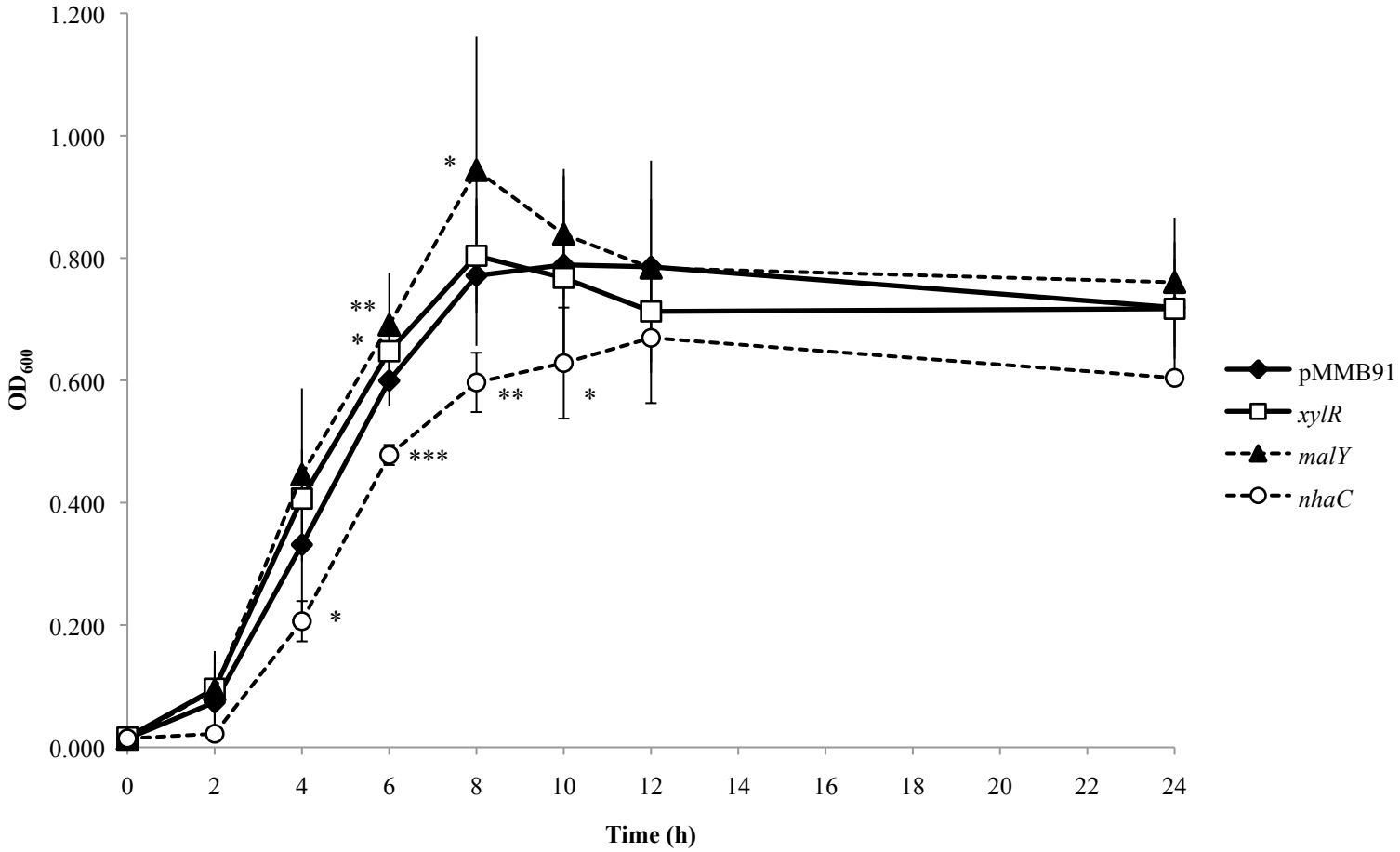


FIG 7 Growth of UTI89 strains overexpressing *xylR* (open square), the *malY* homolog (closed triangle), or *nhaC* (open circle) in human urine. The control strain UTI89(pMMB91) (closed diamond) is also shown. Cultures were shaken at 37°C and 250 rpm for 24 h in sterile pooled human urine with 40 μg/ml kanamycin and 0.33 mM IPTG. Each data point represents the mean ± SD from at least 5 replicates. The following denotes significant P values: * $P < 0.05$, ** $P < 0.01$, *** $P < 0.0001$.

(UTI89, P = 0.00003; UTI89 Δ*omrAB*, P = 0.00003), but estimated xylose concentrations of culture supernatant did not differ significantly between the two strains cultured to mid-log phase (P = 0.18) or overnight (P = 0.43). Although the Δ*omrAB* mutation did not appear to have an effect on the xylose concentration, these results indicate that both strains utilized xylose during growth in human urine.

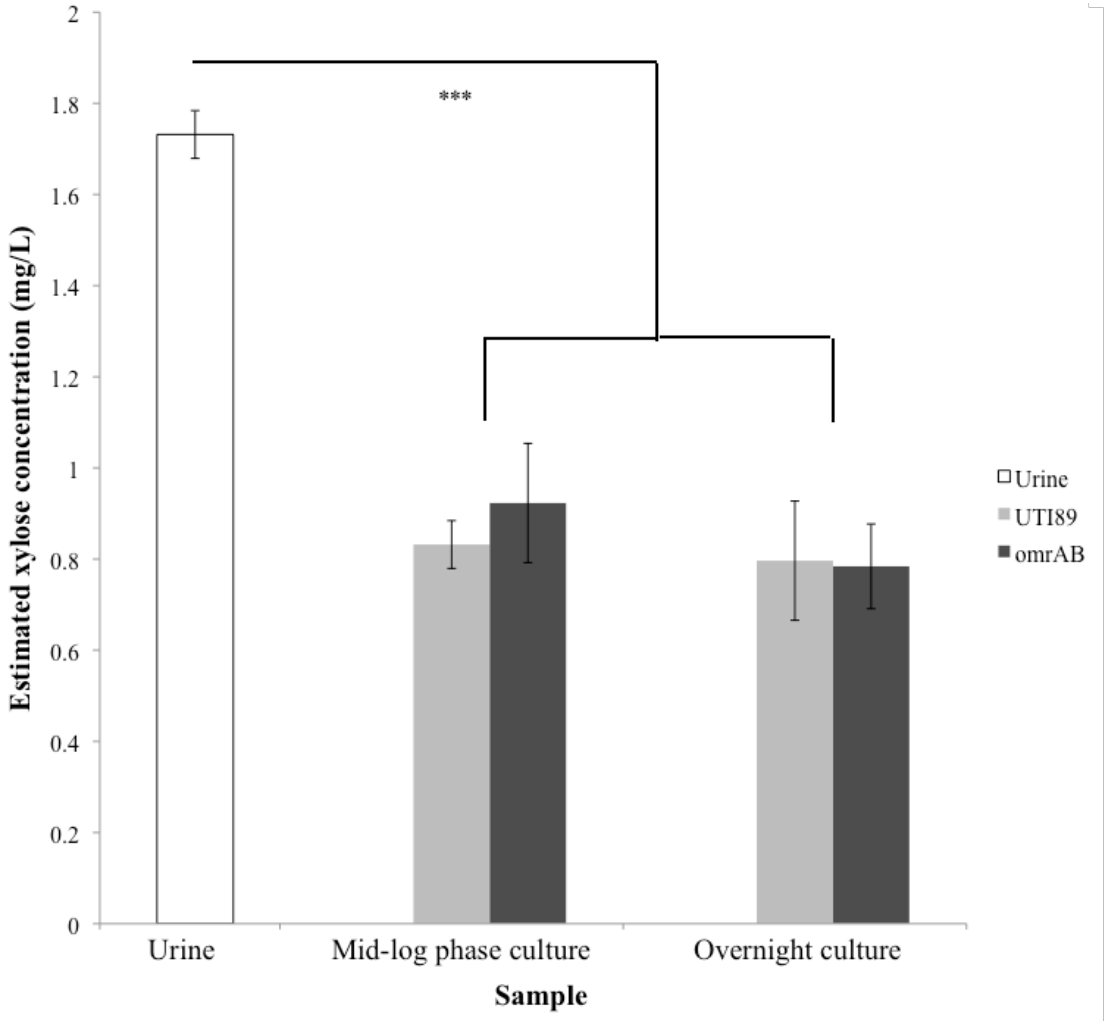


FIG 8 Estimated xylose concentrations of UTI89 and UTI89 Δ*omrAB* cultures grown in human urine to mid-log phase (OD_{600} = 0.5) and overnight. The data represent the means ± SD from at least 3 replicates. Significance is represented by the following: *** P < 0.0001.

DISCUSSION

The main objectives of this study were to determine the effects of an Δ*omrAB* mutation on transcript abundance in UPEC strain UTI89 grown in human urine and to determine if genes affected by the Δ*omrAB* mutation affect the ability of UTI89 to grow in human urine. Our results indicate that OmrAB affect transcript abundance of a variety of genes, and that two hypothetical protein genes, *nhaC* and a *malY* homolog, as well as the *xyl* regulon activator *xylR*, affect UTI89 growth in human urine when overexpressed.

UPEC survival in osmotically stressful, nutrient-poor, urine-saturated environments is important for the establishment of UTIs. Under such harsh environmental conditions, bacteria often utilize sRNAs to modulate expression of genes related to stress and virulence (31, 32). In *E. coli*, OmpR transcriptionally induces the redundant sRNA genes *omrA* and *omrB* under high osmolarity conditions. In turn, OmrAB regulate the EnvZ/OmpR two-component osmoregulatory system (29, 43) as well as other targets involved in motility and adherence (44-47). RNAseq analysis in this study showed that an *omrAB* deletion had a significant effect on the transcriptome of UPEC strain UTI89 grown in human urine. A previous study has indicated that the deletion of *omrAB* from the genome of NU149 reduced its fitness in a mouse model; some of the changes in transcript abundance observed in this study may reflect that attenuation (48).

Broad effects of an *omrAB* deletion on the transcriptome of UTI89 grown in urine

RNAseq analysis indicated significant dysregulation in the transcript levels of over 400 genes of UTI89 Δ*omrAB* grown in human urine compared to UTI89 cultures grown in human urine. The 80 genes with the most statistically significant differences in transcript abundance between the two strains belonged to a broad range of functional groups (Table 3). Genes involved in carbohydrate metabolism and transport, specifically those involved in xylose metabolism, displayed some of the largest fold-differences in transcript levels between wild-type and mutant strains. UTI89 Δ*omrAB* showed both increased and decreased transcript levels of xylose, maltose, and mannose metabolism genes relative to the parent strain. One study showed that the dysfunction of genes involved in carbohydrate metabolism pathways (*e.g.,* pentose phosphate pathway, glycolysis, Entner Duodoroff pathway) does not affect UPEC fitness during UTI (13), indicating that sugars are not carbon sources for UPEC *in vivo*. However, proteins involved in xylose and fructose metabolism were found to be upregulated in UPEC strain CFT073 in urine cultures compared to general growth medium cultures (16). Surprisingly, a CFT073 Δ*xylA* mutant somewhat outcompeted the parent strain during infection of mouse bladders. Although the RNAseq and qRT-pCR data are somewhat conflicting, our data indicates that xylose metabolism is involved in UPEC growth in urine and *in vivo*.

In addition to carbohydrate metabolism genes, transcript levels of amino acid metabolism and transport genes were dysregulated in UTI89 Δ*omrAB* urine cultures relative to UTI89 urine cultures. Specifically, genes involved in branched-chain amino acid metabolism (*ilvABCDE*, *ilvGMN*, *leuD*), glutamate/glutamine metabolism and

nitrogen assimilation (*gltJKL*, *glnA*), and alanine metabolism (*ddl*) were upregulated in UTI89 Δ*omrAB*. As small peptides and amino acids, specifically branched-chain amino acids, are the main carbon sources for UPEC during UTI and are necessary for full fitness during infection of mice (16), connections between OmrAB and amino acid metabolism indicate that these sRNAs may play a significant role in regulating UPEC carbon metabolism during growth in human urine.

Other genes with transcript levels significantly dysregulated in urine-grown UTI89 Δ*omrAB* encode hypothetical proteins and housekeeping proteins (Table 3). The two hypothetical protein genes that showed significant dysregulation in UTI89 Δ*omrAB* compared to UTI89 were the *malY* homolog and *nhaC*, which will be discussed below. Most of the other hypothetical protein genes are uncharacterized and require further investigation to determine the functions of their products. The RNAseq data also indicated that transcript levels of essential housekeeping genes that encode products such as the DNA polymerase III γ and τ subunits as well as 30S and 50S rRNA genes were downregulated in UTI89 Δ*omrAB*. The nitrogen assimilation controller *nac*, one half of the NtrC/Nac system responsible for upregulation of nitrogen assimilation genes (73), was upregulated in UTI89 Δ*omrAB*. As the RNAseq data indicated the *gltJKL* and *glnA* transcription was upregulated in UTI89 Δ*omrAB* compared to wild-type, indicating that OmrAB may downregulate parts of nitrogen metabolism during UTI89 growth in urine.

Transcript levels of seven genes that encode membrane shock proteins were also significantly upregulated in UTI89 Δ*omrAB* urine cultures. Six of the seven genes belong to the *psp* (phage shock protein) regulon (Table 3). The *psp* regulon is involved in the maintenance of inner membrane integrity and proton motive force, and its expression is

induced upon cellular exposure to a variety of stressors (*e.g.*, osmotic, chemical, or phage stressors; 74). Additionally, *psp* regulon dysfunction has been shown to decrease *E. coli* fitness. If this regulon is indeed regulated by OmrAB, it would add to the number of membrane protein genes that are affected by OmrAB. Furthermore, as the *psp* regulon is induced by high osmolarity, it may be activated and contribute to survival in the osmotically stressful conditions found in urine.

RNAseq and qRT-PCR analyses indicated that transcript levels of genes belonging to the *xyl* operons (*e.g.*, *xylA* and *xylR*) as well as the uncharacterized hypothetical protein genes *nhaC* and the *malY* homolog were upregulated roughly 10-fold and 80- to 100-fold, respectively, in UTI89 Δ*omrAB* grown in human urine relative to the parent strain. Bioinformatic analysis using databases available through the BLAST tool (https://blast.ncbi.nlm.nih.gov/Blast.cgi) suggest that *nhaC* encodes a NhaC Na^+/H^+ antiporter family protein, while the *malY* homolog encodes a maltose operon regulator and cystathionine β-lyase. qRT-PCR indicated that transcript levels of these genes in UTI89 Δ*omrAB* urine cultures differed significantly from those in UTI89 urine cultures, although the differences were less drastic (*i.e.,* 10-fold to 100-fold differences in RNAseq data compared to roughly 2-fold differences in qRT-PCR data) and inverted (*i.e.,* UTI89 exhibited higher transcript levels than UTI89 Δ*omrAB*) relative to the RNAseq data. This discrepancy between the RNAseq and qRT-PCR results may have resulted from variability in urine constituents, osmolality, or even pH, which in turn could affect expression of *omrAB* and other genes in UTI89. These factors also may be the reason that transcript levels of various known OmrAB targets (*e.g.*, OmpR) were not significantly affected in this RNAseq analysis. Future studies may benefit from storing urine samples

for compositional analysis in order to investigate this possibility. However, because both strains used in the RNAseq and qRT-PCR analyses were subjected to the same growth conditions, the presence or absence or *omrAB* appears to be the only obvious cause for transcriptional differences between the strains in both cases.

Effects of *malY* homolog overexpression on UTI89 urine growth

Since transcript levels of *xylR*, *nhaC*, and the *malY* homolog were affected by the *omrAB* deletion during growth in human urine, we examined whether overexpression of these genes in wild-type UTI89 affected its growth in human urine. UTI89 urine cultures overexpressing the *malY* homolog grew to significantly higher OD_{600} values than the parent strain during mid-log phase and late-log phase. As mentioned above, wild-type MalY functions as a cystathionine β-lyase and a *mal* regulon repressor. The UTI89 MalY homolog shares 29% identity and 51% positives matching with MalY of the *E. coli* reference strain K-12. Further, the UTI89 MalY homolog appears to possess the exact residues that are critical for cystathionine β-lyase activity and has none of the mutations that a previous study found to be inhibitory to *mal* repressor activity, although not all residues involved in *mal* repressor activity match those of the *E. coli* K12 MalY protein (75). While experimental results are needed to determine precisely what activities the MalY homolog possesses, the protein sequence analysis performed here indicates that it potentially has both activities found in wild-type MalY.

Studies have indicated that cystathionine β-lyases contribute to virulence of *Salmonella enterica* serovar Gallinarum and *Salmonella enterica* serovar Typhimurium in mice (51, 52) as well as virulence of an avian *E. coli* strain in chicken lungs and spleens (53). However, MalY also acts as a repressor of the *mal* regulon responsible for

maltose transport and metabolism, an activity which has also been linked to bacterial virulence. One study has shown that UPEC strain CFT073 lacking the *metV* pathogenicity island that contains a different maltose regulon repressor gene, *pafR*, as well as a gene likely homologous to *malY* (based on BLAST results), is outcompeted by the parent strain in transurethral infection of mice (54). A subsequent study also indicated that CFT073 Δ*pafR* is outcompeted by the parent strain during coinfection of the bladders and kidneys of mice (55). Additionally, studies haved linked maltose metabolism to cytopathicity in *E. coli* (56), growth of Group A *Streptococcus* in saliva (57), and virulence factor production in *V. cholerae* (58), and found *malX* (*i.e.,* maltose- and glucose-specific transport protein component) to be necessary for full fitness of an avian pathogenic *E. coli* strain during infection of chicken lungs, hearts and kidneys (52). Taken together, these studies indicate that the *mal* regulon repressor activity of the *malY* homolog is likely related to its improving UTI89 growth in human urine when overexpressed.

Previous studies have shown that the dysfunction or deletion of cystathionine β-lyase (*metC*) genes or genes with *mal* regulon repressor (*pafR*) activity inhibit virulence in *E. coli* and other bacteria (51-58). The results of this study indicate that the converse (*i.e.,* overexpression of a *malY* homolog) yields a somewhat complementary effect by improving UTI89 growth in human urine relative to the parent strain. This may be due to increased cystathionine β-lyase activity, increased *mal* regulon repressor activity, or both. We postulate that both increased *mal* regulon repression and cystathionine β-lyase activity may improve the ability of UTI89 to grow in urine when MalY is overexpressed. This is because of the lack of necessity for maltose metabolism due to its relative scarcity

in urine and the necessity for methionine metabolism due to the scarcity of L-methionine and abundance of L-cysteine and L-cystathionine in urine.

Effects of *nhaC* overexpression on UTI89 urine growth

The *nhaC* gene is located directly downstream of the *malY* homolog and has an eight nucleotide overlap with the *malY* ORF. This study found that overexpression of *nhaC* caused UTI89 urine cultures to grow to OD_{600} values significantly lower than those of parent strain urine cultures in early-log, mid-log, and late-log phases (Figure 4). NhaC may be involved in pH homeostasis in environments of basic pH based on the characterizations of similar Na^+/H^+ antiporters (49). Na^+/H^+ antiporters generally import H^+, thus contributing to acidification of the cytoplasm. Because tight regulation of Na^+/H^+ antiporter genes is required for growth in a variety of environments, loss of expression or overexpression of the *nhaC* gene would likely be harmful to UPEC. If NhaC contributes to cytoplasm acidification in UTI89, it would be unfavorable for UPEC cells to overexpress this protein during growth in acidic urine, potentially explaining the growth defects observed throughout the log-phase growth of UTI89 overexpressing *nhaC* in this study. Further study is necessary to determine what metabolites or ions NhaC transports. One possibility is that NhaC is used to import sulfate and/or an intermediate in the cysteine and methionine metabolism for use in synthesis of both amino acids. If so, this would connect *nhaC* and the *malY* homolog and explain why the two genes appear to be co-transcribed (*i.e., nhaC* imports sulfate, L-cysteine, or L-cystathionine for use in methionine metabolism, and the *malY* homolog converts L-cystathionine to L-homocysteine). Further, it would tie *nhaC* to the metabolism of amino acids, which are the central carbon source of UPEC *in vivo* (13).

Interestingly, the *nhaC* and *malY* homolog genes are found within the *leuX*-associated pathogenicity island II of strain UTI89. The UPEC strains 536 (76) and NU14 (77) as well as an O25b:H4 cystitis isolate (78) and other extraintestinal pathogenic *E. coli* isolates identified using the online BLAST tool (https://blast.ncbi.nlm.nih.gov) also contain *nhaC* and the *malY* homolog in their genomes. However, strain CFT073 has neither the *nhaC* nor the *malY* homolog genes in its genome, which must have been lost after the evolutionary bifurcation of strains CFT073 and 536 (79). As previously mentioned, *nhaC* and the *malY* homolog overlap slightly in the UTI89 genome. Additionally, the rho-independent terminator prediction tool ARNold (http://rna.igmors.u-psud.fr/toolbox/arnold/index.php) predicted a terminator sequence after *nhaC* but not the *malY* homolog, making it appear that these two genes may produce a biscistronic transcript. This is interesting because, if both MalY homolog and NhaC are translated from the same mRNA, one would expect both genes products to be expressed or repressed under the same conditions and have similar effects on UTI89 growth in urine. However, the gene products appeared to have somewhat opposite effects on growth of UTI89 in human urine. Further characterization of their functions is necessary to explain their converse effects on UTI89 growth in urine when overexpressed.

Effects of *xylR* overexpression on UTI89 urine growth

The overexpression of *xylR*, the transcriptional activator of the *xyl* regulon (Figure 2), was also tested for an effect on UTI89 growth in human urine. A significant increase in culture density was observed between urine cultures of UTI89 overexpressing *xylR* and parent strain urine cultures at the 6 h time point, although the difference observed was relatively minor. However, this result may be biologically significant in the light of the

previously mentioned studies that found *xyl* genes to be associated with UPEC survival in urine and virulence. These studies observed that UPEC strain CFT073 and an asymptomatic bacteriuria strain exhibited upregulated XylA (xylose isomerase) and *xylFGH* levels, respectively, during growth in human urine compared to growth in general growth medium (16, 18). Additionally, KguS of the KguR/KguS two-component regulatory system, which is necessary for full fitness of strain CFT073 during infection of murine urinary tracts, was found to regulate XylA levels in CFT073 during growth in urine (21), and a CFT073 Δ*xylA* mutant strain outcompeted the parent strain in mouse bladders ($P = 0.0625$) and kidneys ($P = 0.0649$, 16). Despite these data, these studies did not investigate potential connections of *xyl* genes with UPEC urine growth or virulence.

In the present study, UTI89 and UTI89 Δ*omrAB* appeared to utilize xylose during growth in urine, although there was no difference in approximated xylose content of urine culture supernatants between the strains (Figure 8). In general, carbohydrate metabolism is not significant to UPEC cells *in vivo*, as indicated by mutants with deletions of genes involved in pentose phosphate, glycolysis, and Entner-Doudoroff pathways having little effect of UPEC fitness during infection of mice urinary tracts (16). Further, *E. coli* preferentially metabolizes the sugars glucose, lactose, and arabinose before xylose (80). Nevertheless, transcripts and proteins of *xyl* metabolism genes, particularly *xylA*, have been shown to be upregulated during *E. coli* urine growth (16, 18, 21). However, it was shown that a strain CFT073 mutant lacking both the *talA* and *talB* genes, which encode isoenzymes of transaldolase, caused fitness defects during infection of mice (13). This sugar isomerization in the nonoxidative pentose phosphate pathway may be important for UPEC during a UTI to drive nucleotide synthesis (13). The products used by

transaldolase are isomerized from ribulose-5-phosphate and xylulose-5-phosphate (Figure 9). Xylose metabolism may therefore be important during UPEC growth in urine for the replenishment of xylulose-5-phosphate, which is funneled into the nonoxidative pentose phosphate pathway that feeds the synthesis of nucleotide precursors and histidine.

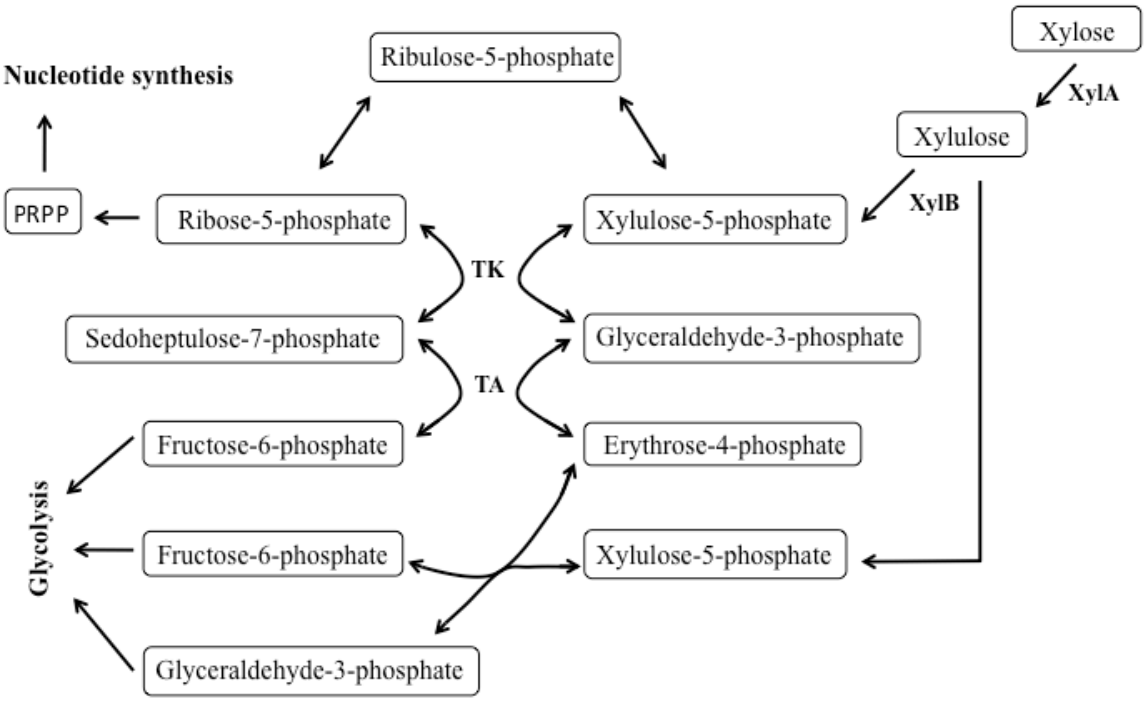


FIG 9 Nonoxidative pentose phosphate pathway and xylose metabolism. TA = transaldolase, TK = transketolase, PRPP = phosphoribosyl pyrophosphate.

We have shown that OmrAB affect the transcript levels of a broad range of genes in UPEC strain UTI89 grown in human urine. Further, we have shown that the OmrAB-regulated genes *xylR*, *nhaC*, and the *malY* homolog affect UTI89 growth in human urine at different times during growth and to different extents. These results add to existing studies that indicate similar genes contribute to the growth or virulence of UPEC or other bacteria. To our knowledge, no previous studies have indicated that OmrAB affect the

transcript levels of any gene investigated in this study. Additional research is necessary to learn whether OmrAB regulate transcript levels of the *xylR*, *nhaC,* and *malY* homolog genes directly or indirectly and to confirm the activities of NhaC and the MalY homolog. If NhaC and the MalY homolog are involved in the import of an important metabolite (*e.g.,* sulfate) and biosynthesis of methionine, they may be potential targets for antibacterial agents. In particular, a potential cystathionine β-lyase may be of interest in this regard due to its dissimilarity to human enzymes and the relative lack of methionine in human urine.

Besides characterization of the hypothetical proteins, it would be desirable for future studies to compositionally analyze urine pools along with transcript levels of UPEC grown in those pools. This would determine whether specific chemical properties or constituents of urine are affecting expression of the genes investigated here. If a specific constituent is found to affect transcript levels of genes of interest, its effect could be analyzed more precisely by growing UPEC in minimal growth medium with varying concentrations of that constituent. Finally, prompt use of urine pools would rule out the possibility that compounds like carbohydrates or peptides are breaking down over time and thereby adding to potential variability of the growth medium.

REFERENCES

1. Foxman B, Barlow R, D'Arcy H, Gillespie B, Sobel JD. 2000. Urinary tract infection: self-reported incidence and associated costs. Ann Epidemiol 10:509–515.

2. Hunstad DA, Justice SS. 2010. Intracellular lifestyles and immune evasion strategies of uropathogenic *Escherichia coli*. Annu Rev Microbiol 64:203–221.

3. Flores-Mireles AL, Walker JN, Caparon M, Hultgren SJ. 2015. Urinary tract infections: epidemiology, mechanisms of infection and treatment options. Nat Rev Microbiol 13:269–284.

4. Foxman B. 2014. Urinary tract infection syndromes. Infect Dis Clinics N America 28:1–13.

5. Wood D, Greenwell T. 2010. Surgical anatomy of the kidney and ureters. Surgery (Oxford) 28:314–316.

6. Patel AK, Chapple CR. 2008. Anatomy of the lower urinary tract. Surgery (Oxford) 26:127–132.

7. Rosen DA, Hooton TM, Stamm WE, Humphrey PA, Hultgren SJ. 2007. Detection of intracellular bacterial communities in human urinary tract infection. PLoS Med 4:e329.

8. Khandelwal P, Abraham SN, Apodaca G. 2009. Cell biology and physiology of the uroepithelium. AJP: Renal Phys 297:1477–1501.

9. Kucheria R. 2005. Urinary tract infections: new insights into a common problem. Postgrad Med J 81:83–86.

10. Mundt LA, Graff L, Shanahan K. 2011. Graff's textbook of routine urinalysis and body fluids. Second ed. Wolters Kluwer/lippincott Williams & Wilkins Health, Philadelphia, PA.

11. Suckow MA, Danneman P, Brayton C. 2001. The laboratory mouse. CRC Press, Boca Raton, FL.

12. Wu XR, Lin JH, Walz T, Häner M, Yu J, Aebi U, Sun TT. 1994. Mammalian uroplakins. A group of highly conserved urothelial differentiation-related membrane proteins. J Biol Chem 269:13716–13724.

13. Alteri CJ, Mobley HL. 2015. Metabolism and fitness of urinary tract pathogens. Microbiol Spectr 3:215–230.

14. Greene SE, Hibbing ME, Janetka J, Chen SL, Hultgren SJ. 2015. Human urine decreases function and expression of type one pili in uropathogenic *Escherichia coli*. mBio 6:e00820-15.

15. Parkkinen J, Virkola R, Korhonen T. 1988. Identification of factors in human urine that inhibit the binding of *Escherichia coli* adhesins. Infect Immun 56:2623–2630.

16. Alteri CJ, Smith SN, Mobley HLT. 2009. Fitness of *Escherichia coli* during urinary tract infection requires gluconeogenesis and the TCA cycle. PLoS Pathogens 5(5):e1000448.

17. Song S, Park C. 1997. Organization and regulation of the D-xylose operons in *Escherichia coli* K-12: XylR acts as a transcriptional activator. J Bacteriol 179:7025–7032.

18. Roos V, Ulett GC, Schembri MA, Klemm P. 2006. The asymptomatic bacteriuria *Escherichia coli* strain 83972 outcompetes uropathogenic *E. coli* strains in human urine. Infect Immun 74:615–624.

19. Takasaki Y, Kosugi Y, Kanbayashi A. 1969. Studies on sugar-isomerizing enzyme purification, crystallization and some properties of glucose isomerase from *Streptomyces* sp. Agric Biol Chem 33:1527–1534.

20. Di Luccio E, Petschacher B, Voegtli J, Chou H-T, Stahlberg H, Nidetzky B, Wilson DK. 2007. Structural and kinetic studies of induced fit in xylulose kinase from *Escherichia coli*. J Mol Biol 365:783–798.

21. Cai W, Wannemuehler Y, Dell'Anna G, Nicholson B, Barbieri NL, Kariyawasam S, Feng Y, Logue CM, Nolan LK, Li G. 2013. A novel two-component signaling system facilitates uropathogenic *Escherichia coli*'s ability to exploit abundant host metabolites. PLoS Pathog 9:e1003428.

22. Bouatra S, Aziat F, Mandal R, Guo AC, Wilson MR, Knox C, Bjorndahl TC, Krishnamurthy R, Saleem F, Liu P, Dame ZT, Poelzer J, Huynh J, Yallou FS, Psychogios N, Dong E, Bogumil R, Roehring C, Wishart DS. 2013. The human urine metabolome. PLoS ONE 8:e73076.

23. Forst S, Delgado J, Inouye M. 1989. Phosphorylation of OmpR by the osmosensor EnvZ modulates expression of the *ompF* and *ompC* genes in *Escherichia coli*. Proc Natl Acad Sci USA 86:6052–6056.

24. Delgado J, Forst S, Harlocker S, Inouye M. 1993. Identification of a phosphorylation site and functional analysis of conserved aspartic acid residues of OmpR, a transcriptional activator for *ompF* and *ompC* in *Escherichia coli*. Mol Microbiol 10:1037–1047.

25. Pratt LA, Hsing W, Gibson KE, Silhavy TJ. 1996. From acids to *osmZ*: multiple factors influence synthesis of the OmpF and OmpC porins in *Escherichia coli*. Mol Microbiol 20:911–917.

26. Schwan WR. 2009. Survival of uropathogenic *Escherichia coli* in the murine urinary tract is dependent on OmpR. Microbiology 155:1832–1839.

27. Rentschler AE, Lovrich SD, Fitton R, Enos-Berlage J, Schwan WR. 2013. OmpR regulation of the uropathogenic *Escherichia coli fimB* gene in an acidic/high osmolality environment. Microbiology 159:316–327.

28. Yamamoto K, Nagura R, Tanabe H, Fujita N, Ishihama A, Utsumi R. 2000. Negative regulation of the bolA1p of *Escherichia coli* K-12 by the transcription factor OmpR for osmolarity response genes. FEMS Microbiol Lett 186:257–262.

29. Brosse A, Korobeinikova A, Gottesman S, Guillier M. 2016. Unexpected properties of sRNA promoters allow feedback control via regulation of a two-component system. Nucleic Acids Res. 44(20):9650-9666.

30. Quinn HJ, Cameron ADS, Dorman CJ. 2014. Bacterial regulon evolution: distinct responses and roles for the identical OmpR proteins of *Salmonella typhimurium* and *Escherichia coli* in the acid stress response. PLoS Genetics 10:e1004215.

31. Gottesman S, Storz G. 2011. Bacterial small RNA regulators: versatile roles and rapidly evolving variations. CSH Perspect Biol 3:a003798–a003798.

32. De Lay N, Schu DJ, Gottesman S. 2013. Bacterial small RNA-based negative regulation: Hfq and its accomplices. J Biol Chem 288:7996–8003.

33. Thomason MK, Storz G. 2010. Bacterial antisense RNAs: How many are there, and what are they doing? Ann Rev Genet 44:167–188.

34. Skippington E, Ragan MA. 2012. Evolutionary dynamics of small RNAs in 27 *Escherichia coli* and *Shigella* genomes. Genome Biol Evol 4:330–345.

35. Lenz DH, Mok KC, Lilley BN, Kulkarni RV, Wingreen NS, Bassler BL. 2004. The small RNA chaperone Hfq and multiple small RNAs control quorum sensing in *Vibrio harveyi* and Vibrio cholerae. Cell 118:69–82.

36. Zeng Q, McNally RR, Sundin GW. 2013. Global small RNA chaperone Hfq and regulatory small RNAs are important virulence regulators in *Erwinia amylovora*. J Bacteriol 195:1706–1717.

37. Porcheron G, Habib R, Houle S, Caza M, Lepine F, Daigle F, Masse E, Dozois CM. 2014. The small RNA RyhB contributes to siderophore production and virulence of uropathogenic *Escherichia coli*. Infect Immun 82:5056–5068.

38. Moores A, Chipper-Keating S, Sun L, McVicker G, Wales L, Gashi K, Blomfield IC. 2014. RfaH suppresses small RNA MicA inhibition of *fimB* expression in *Escherichia coli* K-12. J Bacteriol 196:148–156.

39. Coornaert A, Lu A, Mandin P, Springer M, Gottesman S, Guillier M. 2010. MicA sRNA links the PhoP regulon to cell envelope stress. Mol Microbiol 76:467–479.

40. De Lay N, Gottesman S. 2012. A complex network of small non-coding RNAs regulate motility in *Escherichia coli*: sRNA regulation of motility in *Escherichia coli*. Mol Microbiol 86:524–538.

41. Johansen J, Rasmussen AA, Overgaard M, Valentin-Hansen P. 2006. Conserved small non-coding RNAs that belong to the σ^e regulon: role in downregulation of outer membrane proteins. J Mol Biol 364:1–8.

42. Jahandeh N, Ranjbar R, Behzadi P, Behzadi E. 2015. Uropathogenic *Escherichia coli* virulence genes: invaluable approaches for designing DNA microarray probes. Cent European J Urol 68:452–458.

43. Guillier M, Gottesman S. 2006. Remodelling of the *Escherichia coli* outer membrane by two small regulatory RNAs. Mol Microbiol 59:231–247.

44. Schwan WR. 2011. Regulation of *fim* genes in uropathogenic *Escherichia coli*. World J Clin Infect Dis 1(1):17–25.

45. Barnhart MM, Chapman MR. 2006. Curli biogenesis and function. Annu Rev Microbiol 60:131–147.

46. Holmqvist E, Reimgard J, Sterk M, Grantcharova N, Romling U, Wagner E. 2010. Two antisense RNAs target the transcriptional regulator CsgD to inhibit curli synthesis. EMBO J 29:1840–1850.

47. Mika F, Hengge R. 2014. Small RNAs in the control of *rpoS*, *csgD*, and biofilm architecture of *Escherichia coli*. RNA Biol 11:494–507.

48. Wu, I. 2017. Determining the effect of the loss of the small RNAs OmrA and OmrB on type 1 pilus expression in *Escherichia coli*. MS thesis. University of Wisconsin-La Crosse.

49. Padan E, Bibi E, Ito M, Krulwich TA. 2005. Alkaline pH homeostasis in bacteria: New insights. BBA Biomemb 1717:67–88.

50. Lescat M, Reibel F, Pintard C, Dion S, Glodt J, Gateau C, Launay A, Ledda A, Cruvellier S, Tourret J, Tenaillon O. 2014. The conserved *nhaaR* operon is drastically divergent between b2 and non-b2 *Escherichia coli* and is involved in extra-intestinal virulence. PLoS ONE 9:e108738.

51. Ejim LJ, D'Costa VM, Elowe NH, Loredo-Osti JC, Malo D, Wright GD. 2004. Cystathionine β-lyase is important for virulence of *Salmonella enterica* serovar typhimurium. Infect Immun 72:3310–3314.

52. Li G, Laturnus C, Ewers C, Wieler LH. 2005. Identification of genes required for avian *Escherichia coli* septicemia by signature-tagged mutagenesis. Infection and Immunity 73:2818–2827.

53. Shah DH, Shringi S, Desai AR, Heo E-J, Park J-H, Chae J-S. 2007. Effect of *metC* mutation on *Salmonella* Gallinarum virulence and invasiveness in 1-day-old White Leghorn chickens. Vet Microbiol 119:352–357.

54. Lloyd AL, Henderson TA, Vigil PD, Mobley HLT. 2009. Genomic islands of uropathogenic *Escherichia coli* contribute to virulence. J Bacteriol 191:3469–3481.

55. Baum M, Watad M, Smith SN, Alteri CJ, Gordon N, Rosenshine I, Mobley HL, Amster-Choder O. 2014. PafR, a novel transcription regulator, is important for pathogenesis in uropathogenic *Escherichia coli*. Infect Immun 82:4241–4252.

56. Kumar SS, Sankaran K, Haigh R, Williams PH, Balakrishnan A. 2001. Cytopathic effects of outer-membrane preparations of enteropathogenic *Escherichia coli* and co-expression of maltoporin with secretory virulence factor, EspB. J Med Microbiol 50:602–612.

57. Shelburne SA, Keith DB, Davenport MT, Horstmann N, Brennan RG, Musser JM. 2008. Molecular characterization of group A *Streptococcus* maltodextrin catabolism and its role in pharyngitis. Mol Microbiol 69:436–452.

58. Lång H, Jonson G, Holmgren J, Palva ET. 1994. The maltose regulon of *Vibrio cholerae* affects production and secretion of virulence factors. Infect Immun 62:4781–4788.

59. Ewers C, Dematheis F, Singamaneni HD, Nandanwar N, Fruth A, Diehl I, Semmler T, Wieler LH. 2014. Correlation between the genomic *o454-nlpD* region polymorphisms, virulence gene equipment and phylogenetic group of extraintestinal *Escherichia coli* (ExPEC) enables pathotyping irrespective of host, disease and source of isolation. Gut Pathog 6:37.

60. Mulvey MA, Schilling JD, Hultgren SJ. 2001. Establishment of a persistent *Escherichia coli* reservoir during the acute phase of a bladder infection. Infect Immun 69:4572–4579.

61. Chen SL, Hung C-S, Xu J, Reigstad CS, Magrini V, Sabo A, Blasiar D, Bieri T, Meyer RR, Ozersky P, Armstrong JR, Fulton RS, Latreille JP, Spieth J, Hooton TM, Mardis ER, Hultgren SJ, Gordon JI. 2006. Identification of genes subject to positive selection in uropathogenic strains of *Escherichia coli*: a comparative genomics approach. Proc Natl Acad Sci USA 103:5977–5982.

62. Datsenko KA, Wanner BL. 2000. One-step inactivation of chromosomal genes in *Escherichia coli* K-12 using PCR products. Proc Natl Acad Sci USA 97:6640–6645.

63. Fürste JP, Pansegrau W, Frank R, Blöcker H, Scholz P, Bagdasarian M, Lanka E. 1986. Molecular cloning of the plasmid RP4 primase region in a multi-host-range tacP expression vector. Gene 48:119–131.

64. Lisitsyn N, Lisitsyn N, Wigler M. 1993. Cloning the Differences Between Two Complex Genomes. Science 259:946–951.

65. Stead MB, Agrawal A, Bowden KE, Nasir R, Mohanty BK, Meagher RB, Kushner SR. 2012. RNAsnap : a rapid, quantitative and inexpensive method for isolating total RNA from bacteria. Nucleic Acids Res 40:e156–e156.

66. Livak KJ, Schmittgen TD. 2001. Analysis of relative gene expression data using real-time quantitative PCR and the $2^{-\Delta\Delta Ct}$ method. Methods 25:402–408.

67. Pfaffl M, Horgan G, Dempfle L. 2002. Relative expression software tool (REST©) for group-wise comparison and statistical analysis of relative expression results in real-time PCR. Nucleic Acids Res 30:e36.

68. Schwan WR, Lee JL, Lenard FA, Matthews BT, Beck MT. 2002. Osmolarity and pH growth conditions regulate *fim* gene transcription and type 1 pilus expression in uropathogenic *Escherichia coli*. Infect Immun 70(3):1391-1402.

69. Eberts TJ, Sample RH, Glick MR, Ellis GH. 1979. A simplified, colorimetric micromethod for xylose in serum or urine, with phloroglucinol. Clin Chem 25:1440–1443.

70. Hermida C, Martínez-Costa OH, Corrales G, Teruel C, Sánchez V, Sánchez JJ, Sarrión D, Ariza MJ, Codoceo R, Calvo I, Fernández-Mayoralas A, Aragón JJ. 2014. Improvement and validation of D-xylose determination in urine and serum as a new tool for the noninvasive evaluation of lactase activity in humans. J Clin Lab Anal 28:478–486.

71. Trinder P. 1975. Micro-determination of xylose in plasma. Analyst 100:12-155.

72. Revie D, Smith DW, Yee T. 1988. Kinetic analysis for optimization of DNA ligation reactions. Nuc Acid Res 16(21):10301–10321.

73. Zimmer DP, Soupene E, Lee HL, Wendisch VF, Khodursky AB, Peter BJ, Bender RA, Kustu S. 2000. Nitrogen regulatory protein C-controlled genes of *Escherichia coli*: Scavenging as a defense against nitrogen limitation. Proc Natl Acad Sci USA 97(26):14674–14679.

74. Joly N, Engl C, Jovanovic G, Huvet M, Toni T, Sheng X, Stumpf MPH, Buck M. 2010. Managing membrane stress: the phage shock protein (Psp) response, from molecular mechanisms to physiology. FEMS Microbiol Rev 34:797–827.

75. Zhang L, Jiang W, Nan J, Almqvist J, Huang Y. 2014. The *Escherichia coli* CysZ is a pH dependent sulfate transporter that can be inhibited by sulfite. BBA Biomemb 1838:1809–1816.

76. Hacker J, Knapp S, Goebel W. 1983. Spontaneous deletions and flanking regions of the chromosomally inherited hemolysin determinant of an *Escherichia coli* O6 strain. J Bacteriol 154:1145–1152.

77. Hultgren SJ, Schwan WR, Schaeffer AJ, Duncan JL. 1986. Regulation of production of type 1 pili among urinary tract isolates of *Escherichia coli*. Infect Immun 54:613–620.

78. Alyamani EJ, Khiyami MA, Booq RY, Bahwerth FS, Vaisvil B, Schmitt DP, Kapatral V. 2016. Genome sequence and comparative pathogenic determinants of multidrug resistant uropathogenic *Escherichia coli* O25b:H4, a clinical isolate from Saudi Arabia. J Pure Appl Microbiol 10(4): 2475-2484.

79. Schwan WR, Briska A, Stahl B, Wagner TK, Zentz E, Henkhaus J, Lovrich SD, Agger WA, Callister SM, DuChateau B, Dykes CW. 2010. Use of optical mapping to sort uropathogenic *Escherichia coli* strains into distinct subgroups. Microbiology 156:2124–2135.

80. Aidelberg G, Towbin BD, Rothschild D, Dekel E, Bren A, Alon U. 2014. Hierarchy of non-glucose sugars in *Escherichia coli*. BMC Syst Biol 8(133).